UNIVERSITY OF CALIFORNIA SAN DIEGO

VAX1 and SIX3 within Kisspeptin Neurons Regulate *Kiss1* Gene Expression and the Reproductive Axis

A dissertation submitted in partial satisfaction of the requirements for the degree Doctor of Philosophy

in

Biomedical Sciences

by

Shanna Newton Lavalle

Committee in Charge:

Professor Pamela Mellon, Chair
Professor Alexander Kauffman
Professor Mark Lawson
Professor Mana Parast
Professor Nicholas Webster

2021

The dissertation of Shanna Newton Lavalle is approved, and it is acceptable in quality and form for publication on microfilm and electronically.

University of California San Diego
2021

DEDICATION

This dissertation is dedicated to my Grandmas: Sara Sanchez and Jill Newton, both of whom passed away at the beginning of this year, and Toni Allen, whom I lost when I was young. I know that they would be extremely proud to see the first member of their families receive a doctoral degree. I would also like to dedicate my dissertation to my Grandpa John Sanchez, who was beyond proud when I told him that I would be getting my PhD.

EPIGRAPH

Tranquil as a forest
But on fire within
Once you find your center
You are sure to win

You're unsuited for the rage of war
So pack up, go home, you're through
How could I make a man out of you?

You must be swift as the coursing river
With all the force of a great typhoon
With all the strength of a raging fire
Mysterious as the dark side of the moon

Walt Disney's Mulan
Songwriters: Mathew Wilder and David Zippel

TABLE OF CONTENTS

LIST OF ABBREVIATIONS

ARC	Arcuate nucleus
AVPV	Anteroventral periventricular nucleus
E2	Estradiol
FSH	Follicle-stimulating hormone
GnRH	Gonadotropin-releasing hormone
LH	Luteinizing hormone
Six3	Sine oculis homeobox homolog 3
Vax1	Ventral anterior homeobox 1

LIST OF FIGURES

ACKNOWLEDGEMENTS

I would like to thank my thesis advisor, Pamela Mellon, for her amazing mentorship and guidance. She has helped me develop the skills needed to be a strong scientist and encouraged me to take opportunities that will support my growth. I would also like to acknowledge all of the members of the Mellon Lab who created a wonderful and supportive training environment. Especially, Karen Tonsfeldt who provided day-to-day mentorship and taught me all the nitty-gritty aspects of ensuring scientific rigor in my work, Stephanie Bohaczuk for her insight and mental support, and Ichiko Saotome who quite literally kept our lab running despite all of the challenges that were brought on by the Covid-19 pandemic. I am also extremely grateful for my students, Teresa Chou, Jacqueline Hernandez, and Tiffany Naing. Not only did they help tremendously in the development of these chapters, but mentoring them and watching them grow as scientists and make their own independent marks in the world has been the most rewarding part of this journey. I would also like to thank the members of my thesis committee, Mana Parast, Mark Lawson, Alexander Kauffman, and Nick Webster for their advice, insight, and guidance.

I would also like to acknowledge the Endocrine Society's FLARE program and the members of the Endocrine Society's Trainee Career Development and Core Committee, especially Lori Raetzman, Tracy Williams, and Kirsta Suggs. My involvement in these programs and committees helped me break from my insecurities and develop the confidence in myself that allowed me to thrive in all aspects of my scientific career development. I would also like to thank my undergraduate research advisor, Ashley Carter, for introducing me to the world of research, encouraging me to participate in several undergraduate research programs, and helping me recognize, not only that being a scientist is a viable career, but that it is a perfectly suited to sustain my constant quest of knowledge.

I am extremely thankful for the constant support of my husband, Miguel Lavalle. We met my first year of graduate school and he has since listened to hundreds of hours of practice presentations throughout the years and has provided the emotional support and motivation to

keep me from breaking during my most difficult times. I am grateful for the unconditional love and companionship that Diesel and Maya have provided to me. I would also like to acknowledge my sisters, Sara Newton-Mahony, Elora Newton, and Arbie Newton, who inspire me to be the best version of myself and are always there to make me smile. Finally, I am eternally grateful to my parents, Patty Newton and Robert Newton, who taught me that there are no limits to what I am capable of as long as I work hard and never give up. This mindset has gotten me through my undergraduate and graduate careers and has made this degree possible.

Chapter 1 has been accepted for publication to *Molecular and Cellular Endocrinology*. (Lavalle, Shanna N.; Chou, Teresa; Hernandez, Jacqueline; Naing, Nay Chi P.; Tonsfeldt, Karen J.; Hoffmann, Hanne M; Mellon, Pamela L. 2021. *Kiss1* is differentially regulated in male and female mice by the homeodomain transcription factor VAX1. *Molecular and Cellular Endocrinology* [In Press]. The dissertation author was the primary investigator and author of this paper. Teresa Chou, Jacqueline Hernandez, and Nay Chi Naing provided technical assistance. Karen Tonsfeldt provided technical assistance and assisted with paper composition. Hanne Hoffmann assisted with conceptualization and paper composition. Pamela Mellon supervised the project and provided advice.

Chapter 2 has been submitted for publication to *Endocrinology*. (Lavalle, Shanna N.; Chou, Teresa; Hernandez, Jacqueline; Naing, Nay Chi P.; He, Michelle Y.; Tonsfeldt, Karen J.; Mellon, Pamela L. Deletion of the homeodomain gene *Six3* from kisspeptin neurons causes subfertility in female mice). The dissertation author was the primary investigator and will be the author of this paper. Teresa Chou, Jacqueline Hernandez, Nay Chi Naing, and Michelle He provided technical assistance. Karen Tonsfeldt provided technical assistance and assisted with paper composition. Pamela Mellon supervised the project and provided advice.

VITA

2013 Bachelor of Science, Biology, California State University Long Beach

2021 Doctor of Philosophy, University of California San Diego

PUBLICATIONS

Lavalle, Shanna N.; Chou, Teresa; Hernandez, Jacqueline; Naing, Nay Chi P.; Tonsfeldt, Karen J.; Hoffmann, Hanne M; Mellon, Pamela L. 2021. *Kiss1* is differentially regulated in male and female mice by the homeodomain transcription factor VAX1. *Molecular and Cellular Endocrinology* [In Press].

McKee, Amberle A.; **Newtons, Shanna M.**, Carter, Ashley J.R. 2014. Influence of inbreeding on female mate choice in two species of *Drosophila*. Journal of Insect Behavior. *27*(5), 613–625. https://doi.org/10.1007/s10905-014-9453-5.

ABSTRACT OF DISSERTATION

VAX1 and SIX3 within Kisspeptin Neurons Regulate *Kiss1* Gene Expression and the Reproductive Axis

by

Shanna Newton Lavalle

Doctor of Philosophy in Biomedical Sciences

University of California San Diego, 2021

Professor Pamela Mellon, Chair

Kisspeptin neurons, located in the anteroventral periventricular nucleus (AVPV) and arcuate nucleus (ARC) of the hypothalamus, serve as critical regulators of reproduction, mediating puberty onset, ovulation, and pulsatile gonadotropin-releasing hormone/luteinizing hormone (LH) secretion. Homeodomain transcription factors, such as VAX1 and SIX3, have been implicated in fertility, although the role of these proteins in regulating kisspeptin neuron activity and *Kiss1* gene expression is unclear. I have demonstrated that VAX1 differentially regulates

Kiss1 gene expression in the ARC of male versus female mice and that the loss of *Vax1* from kisspeptin neurons results in a reduction of *Kiss1*-positive cells at the time of the pre-ovulatory LH surge. I have also found that kisspeptin-specific SIX3 is necessary for estrous cyclicity and maximal fecundity in female mice and that SIX3 differentially regulates the mouse and human *Kiss1/KISS1* promoters *in vitro* and can act as repressor of *cFos* transcription *in vitro* and *in vivo*. This work provides context for the specific roles that homeodomain transcription factors play within kisspeptin neurons and their implications in fertility.

Chapter 1: *Kiss1* is differentially regulated in male and female mice by the homeodomain transcription factor VAX1

Abstract

Regulation of *Kiss1* transcription is crucial to the development and function of the reproductive axis. The homeodomain transcription factor, ventral anterior homeobox (VAX1), has been implicated as a potential regulator of *Kiss1* transcription. However, it is unknown whether VAX1 directly mediates transcription within kisspeptin neurons or works indirectly by acting upstream of kisspeptin neuron populations. This study tested the hypothesis that VAX1 within kisspeptin neurons regulates *Kiss1* gene expression. We found that VAX1 acts as a repressor of *Kiss1 in vitro* and within the male arcuate nucleus *in vivo*. In female mice, we found that the loss of VAX1 caused a reduction in *Kiss1* expression and *Kiss1*-containing neurons in the anteroventral periventricular nucleus at the time of the preovulatory luteinizing hormone surge, but was compensated by an increase in *Kiss1-cFos* colocalization. Despite changes in *Kiss1* transcription, gonadotropin levels were unaffected and there were no impairments to fertility.

Introduction

Kisspeptin, encoded by the *Kiss1* gene, is a critical peptide hormone in the reproductive neuroendocrine axis. Kisspeptin, released from neurons in the anteroventral periventricular nucleus (AVPV) and arcuate nucleus (ARC), directly stimulates gonadotropin-releasing hormone (GnRH) release by binding to its receptor (Kiss1R) located on GnRH neurons (1-5). GnRH, in turn, stimulates the gonadotrope cells of the pituitary to release luteinizing hormone (LH) and follicle-stimulating hormone (FSH) to regulate ovulation, folliculogenesis, and the synthesis of gonadal sex steroids (6-8). Disruptions to kisspeptin signaling by mutations in the *Kiss1* and *Kiss1R* genes, in both mice and humans, lead to impairments in sexual maturation, gonadotropin and sex steroid secretion, and fertility (9-12).

Kiss1 expression in the AVPV and ARC is differentially regulated by sex steroid feedback, leading to divergent roles in reproductive function. Many ARC kisspeptin neurons coexpress the stimulatory peptide, neurokinin B, and the inhibitory peptide, dynorphin, and are thought to be responsible for stimulating basal pulsatile GnRH secretion (5, 13-17). Sex steroids, such as androgens, estradiol (E2), and progesterone, are detected by sex steroid receptors on kisspeptin neurons in the ARC and produce a negative feedback response resulting in decreased *Kiss1* expression and decreased LH pulse frequency (18-20). Conversely, AVPV kisspeptin neurons, which are sexually dimorphic and primarily found in females, increase *Kiss1* expression in response to E2 (18). This positive feedback, along with increased neuronal activity, is necessary for increased GnRH secretion, leading to the induction of the LH surge that prompts ovulation (21, 22).

Recently, several homeodomain transcription factors have emerged as critical regulators of the reproductive axis, yet little is known of their influence on kisspeptin signaling (23-28). Ventral anterior homeobox 1 (VAX1) is a highly conserved homeodomain transcription factor, with the amino acid sequence of the homeodomain binding domain identical between mouse and human, and was first recognized for its importance in the development of the rostral and ventral forebrain (29). In mice, *Vax1* is expressed in the olfactory placode, hypothalamus, pituitary, and the testis, but not the ovary (24). VAX1 has recently been implicated as a crucial regulator of reproduction. The loss of a single *Vax1* allele in the *Vax1* heterozygous animal reduces the number of GnRH-expressing neurons by half, and results in reproductive deficiencies, such as a reduction in total sperm and sperm motility in males and increased estrous cycle length in females (24, 30). Complete loss of *Vax1* results in no detectable GnRH-expressing cells, demonstrating a gene-dose dependent role of VAX1 (30). Selective deletion of VAX1 from GnRH neurons abolishes GnRH expression, resulting in hypogonadism and complete infertility in both male and female mice (25, 30), while VAX1 in the suprachiasmatic nucleus (SCN) regulates the LH surge (26). However, these additional studies, do not fully explain the reproductive phenotypes

observed in *Vax1* heterozygous females. While the importance of *Vax1* expression within GnRH neurons and the SCN has been demonstrated (25, 26, 31), the role of *Vax1* in other regions and cell types within the hypothalamus has largely been unexplored.

Haploinsufficiency of *Vax1* in heterozygous females leads to a robust increase in *Kiss1* mRNA levels in the AVPV and a corresponding increase in circulating LH and E2 (24), which was not observed in mice with selective deletion of *Vax1* in GnRH neurons (30). Several regions of both mouse and human *Kiss1/KISS1* promoters contain the VAX1 consensus sequence (ATTA), yet it is unknown whether the increased *Kiss1* transcription is due to a direct effect of VAX1 at the level of the kisspeptin neurons, or an indirect effect through altered steroid feedback to kisspeptin neurons. Additionally, it is unknown whether a homozygous loss of *Vax1* within ARC kisspeptin neurons would lead to a change in *Kiss1* gene expression. Our current study aims to test the hypothesis that VAX1 contributes to the regulation of *Kiss1* transcription in ARC and AVPV kisspeptin populations and consequently regulates gonadotropin secretion. To address our hypothesis, we used immortalized kisspeptin cell lines, as well as transgenic mouse models with VAX1 deleted from *Kiss1*-expressing cells. We found that VAX1 regulates the human *KISS1* promoter *in vitro* and *Kiss1* transcription *in vivo*, but the loss of VAX1 from *Kiss1*-expressing cells *in vivo* does not alter fertility.

Methods

Animals

All animal procedures were performed in accordance with the University of California, San Diego Institutional Animal Care and Use Committee regulations. To produce mice lacking VAX1 in kisspeptin cells, we crossed $Vax1^{Flox/Flox}$ mice (RRID:MGI:6500817) (30) with $Kiss1^{Cre}$ mice (RRID:IMSR_JAX:023426) (32). Offspring were backcrossed to generate $Vax1^{Flox/Flox}$:$Kiss1^{Cre}$ conditional knockouts ($Vax1^{KissCre}$) or $Vax1^{Flox/Flox}$:$Kiss1^{WT}$ ($Vax1^{WT}$). $Kiss1^{Cre}$ reporter mice were generated by crossing $Kiss1^{Cre}$ mice with Ai9 Rosa-tdTomato mice (RRID:MGI:104735) (33) to

create mice in which Kiss1^{Cre} expressing cells were identifiable by tdTomato expression. All mice were on a C57BL/6 background, group housed, and maintained on a 12-hour light, 12-hour dark cycle, with *ad libitum* chow and water. Animals were randomly assigned to experimental groups. Mice were sacrificed with CO_2 or isoflurane overdose followed by rapid decapitation. All animals were sacrificed between zeitgeber time (ZT) 4-7, unless otherwise stated. Female mice were sacrificed during diestrus unless otherwise stated.

For genotyping, genomic DNA was extracted from hypothalamus, pituitary, testis, ovary, and tail tip using DNeasy Kit (Qiagen) according to manufacturer's instructions. To differentiate between a Vax1 flox allele and wildtype allele we used the following primers: VaxFlox-Forward: 5'-GCCGGAACCGAAGTTCCTA-3', VaxWT-Forward: 5'-CCAGTAAGAGCCCCTTTGGG-3', and Vax-Reverse: 5'-CGGATAGAC CCCTTGGCATC-3'. To detect *Vax1* recombination, the following primers were used: VaxRec-Forward: 5'-GCAGTGGCCTAGAGAGATCG-3' and VaxRec-Reverse: 5-GCACTGTGTAGTGCTCCTAT-3'. CRE genotyping was performed using CRE-Forward: 5'-GCATTACCGGTCGTAGCAACGAGTG-3' and CRE-Reverse: 5'-GAACGCTAGAGCCTGTTTTGCACGTTC-3'. tdTomato mice were genotyped using tdtF1: 5'-GGCATTAAAGCAGCGTATCC-3', tdtR1: 5;- CTGTTCCTGTACGGCATGG-3, tdtF2: 5'-CCGAAAATCTGTGGGAAGTC-3', tdtR2: 5'- AAGGGAGCTGCAGTGGAGTA-3'. Mice that were positive for germline recombination of VAX1 were excluded from the study.

Immunohistochemistry

Kiss1^{Cre}-tdTomato$^{+/-}$ mice were euthanized at ZT6. Brains were quickly dissected and submerged in 4% PFA overnight. The following day, brains were transferred to 30% sucrose until they sank. 40 µm sections containing the AVPV were sectioned using a cryostat and sections transferred to PBS. On the day of staining, sections underwent heated antigen retrieval in 1X Citra buffer (Biogenex). Sections were washed and processed with a Mouse-on-Mouse ABC kit (Vector Labs) according to manufacturer's instruction. VAX1 antibody (RRID:AB_2723772) (Clone

OTI4E5, Origene) was used at 1:100. After ABC processing for 30 minutes, sections were washed and incubated in 1:250 biotinylated tyramide (Akoya Biosciences) with 0.003% H_2O_2 for ten minutes. Sections were washed again and incubated in 1:200 Streptavidin DyLight 488 (Invitrogen) for 30 minutes. Sections were washed, mounted, and coverslipped with ProLong with DAPI (Invitrogen).

RNA Isolation and qPCR

Brains were collected on dry ice and immediately stored at -80ºC. Two mm AVPV and ARC micropunches were collected on a cryostat from 0.3 mm thick sections as previously described (34, 35). RNA from micropunches was isolated with RNeasy-Micro Kit (Qiagen) according to manufacturer's instructions. Purified RNA was converted to cDNA using iScript cDNA Synthesis Kit (Bio-Rad Laboratories). cDNA products were detected on a Bio-Rad CFX Connect quantitative real-time PCR system (Bio-Rad laboratories) using SYBR Green Supermix (Bio-Rad Laboratories). Data were analyzed by the $2^{-\Delta\Delta Ct}$ method (36), by normalizing the gene of interest to *Gapdh,* and represented as mean fold change compared to $Vax1^{WT}$±SEM. The following primers were used: Kiss1-Forward: 5'-TGCTGCTTCTCCTCTGT-3', Kiss1-Reverse: 5'-ACCGCGATTCCTTTTGC-3' (37), Pdyn-Forward: 5'-GTGTGCAGTGAGGATTCAGG-3', Pdyn-Reverse: 5'-AGTCATCCTTGCCACGGAGC-3' (38), Tac2-Forward: 5'-CTGCTTCGGAGACTCTACG-3', Tac2-Reverse: 5'-GGTTGGCTGTTCCTCTTGC-3' (38), Gapdh-Forward: 5'-TGCACCACCAACTGCTTAG-3', Gapdh-Reverse: 5'-GGATGCAGGGATGATGTTC-3'.

Cell Culture

KTaR-1 (RRID:CVCL_VS93) and KTaV-3 (RRID:CVCL_VS94) cell lines (kindly provided by Patrick E. Chappell, Oregon State University) (39) were maintained in complete medium

consisting of DMEM (Corning) containing 10% fetal bovine serum (FBS) (Omega Scientific) and 1% penicillin/streptomycin (HyClone) and incubated at 37ºC with 5% CO_2.

Hormones

17β-estradiol (E2) was obtained from Sigma-Aldrich (St. Louis, MO). For cell culture, E2 was dissolved in absolute ethanol and diluted to a 1 nM stock. Immediately prior to hormone treatment, 1 nM E2 stock was diluted 1:1000 in charcoal-stripped DMEM to a final concentration of 1 pM E2. For E2 pellets, E2 was dissolved in sesame oil to a concentration of 25 µg/ml. Methyltrienolone (R1881) was obtained from NEN Life Sciences (Boston, MA) and diluted to a 10 mM R1881 stock in absolute ethanol. Immediately prior to hormone treatments, 10 mM stock was diluted 1:1000 in charcoal-stripped DMEM to a final concentration of 10 µM R1881.

Site-Directed Mutagenesis

Site-directed mutagenesis of three regions of the -1313/+27 human-Kiss-Luc in a pGL2 backbone (hKiss-Luc) (40), kindly provided by Alejandro Lomniczi and Sergio Ojeda, (Oregon National Primate Research Center), was performed using the Q5 Site-Directed Mutagenesis Kit (New England Biolabs) according to manufacturer's instructions. The µ-1211-1193 sequence was mutated at -1211 to -1193 base pairs (bp) upstream of the transcriptional start site (TSS) from **TAAT**GGGTGTGA**TAATAAT** to **CGGC**GGGTGTGA**CGGCGGC**. The µ-1111-1108 sequence was mutated at -1111 to -1108 bp upstream of the TSS from **ATTA** to **CGGC**. The µ-362-359 sequence was mutated at -362 to -359 bp upstream TSS from **ATTA** to **CGGC**.

Transient Transfections and Luciferase Assays

One day prior to transfections, KTAR-1 and KTAV-3 cells were seeded at 3 x 10^4 cells per well in 12-well plates with DMEM containing 10% FBS. Transient transfections were performed using Polyjet In Vitro DNA Transfection Reagent (SignaGen Laboratories), following

manufacturer's instructions. For all experiments, each well was transfected with 500 ng of reporter plasmid, -1313/+27 human-Kiss-Luc in a pGL2 backbone (hKiss-Luc) (40) or reporter backbone, pGL2, and co-transfected with VAX1-CMV6 (VAX1) (30) or CMV6-empty vector (EV) (TrueClone, Origene). 100 ng of a reporter plasmid containing β-galactosidase driven by the herpes virus thymidine kinase promoter (TK-βgal) was co-transfected to serve as an internal control for transfection efficiency. To determine optimal VAX1 concentration, 0 to 50 ng VAX1 or EV was co-transfected with reporter plasmids. To determine if VAX1 regulated the *KISS1* promoter through regions containing ATTA sites, we co-transfected hKiss-Luc, μ-1211-1193, μ-1111-1108, and μ-362-359 or pGL2, with 50 ng VAX1 or EV. Polyjet/DNA complex-containing medium was removed after 24 hours and replaced with complete medium. Cells were harvested 48 hours from start of transfection.

For transfections involving hormone treatments, cells were seeded in charcoal-stripped FBS. 50 ng VAX1 or EV was transfected along with 100 ng ratAR-pSG5 (41) or 50 ng ERα-pcDNA3.1 to ensure adequate expression of steroid receptors. Polyjet/DNA complex-containing medium was replaced after 24 hours with charcoal-stripped medium containing 10 μM R1881 (synthetic androgen), 1 pM E2, or vehicle (100% ethanol). Cells were harvested 48 hours following hormone treatment. To harvest cells, medium was aspirated, cells were washed with 1X PBS and then lysed with 0.1 M K-phosphate buffer, pH 7.8, containing 0.2% Triton X-100. Luciferase and β-galactosidase assays were performed as previously described (42). Transfections were performed in triplicate. Within each well, luciferase values were normalized to TK-βgal values. Luciferase/TK-βgal triplicate values were averaged and then hKiss-Luc, μ-1211-1193, μ-1111-1108, and μ-362-359 values were normalized to pGL2 values. A minimum of three independent replicates per experiment were performed.

Hormone Analysis

Blood samples were collected at time of euthanasia, allowed to clot at room temperature for 1 hour, centrifuged at 2000 ×g for 15 minutes, and then serum was collected and stored at -20ºC until assayed. Serum LH, FSH, estradiol, and testosterone were measured by The University of Virginia Center for Research in Reproduction Ligand Assay and Analysis Core. LH was measured using LH RIA with a reportable range between 0.02 – 75.0 ng/mL (Intra-assay CV=5.5%, Inter-assay CV=8.4%). FSH was measured using FSH RIA with a reportable range between 3.0 – 75.0 ng/mL (Intra-assay CV=6.7%, Inter-assay CV=8.7%). Estradiol was measured using an ELISA with reportable range between 3.0 – 300.0 pg/mL (Intra-assay CV=7.5%, Inter-assay CV=10.1%). Testosterone was measured using an ELISA with reportable range between 10.0 – 1600.0 ng/dL (Intra-assay CV=6.0%, Inter-assay CV=9.3%).

LH Surge

Between ZT 2 - 5, female mice (10-16 weeks old, weighing between 18-28 grams) were ovariectomized and a pellet containing 0.75 µg of 17-β estradiol dissolved in sesame oil subcutaneously implanted to mimic proestrus levels of E2 (21). Two days after surgery, mice were sacrificed either in the morning (AM), between ZT 4-5, or at the time of lights off (PM), between ZT 12-13. Blood and brains were collected at sacrifice. An LH surge was conservatively defined as LH values that were 3 standard deviations above the AM average (22).

Fluorescent In Situ Hybridization (ISH)

20 µm serial coronal sections were collected from fresh frozen brains, spanning the length of the AVPV or ARC (34, 35). Sections were fixed in chilled 4% PFA, washed two times with 1X PBS, and dehydrated through a series of ethanol washes ranging from 50%-100% ethanol. RNAscope Multiplex Fluorescent v2 Assay (Advanced Cell Diagnostic, 323100) was performed according to manufacturer's instructions with the following probes: Mm-Kiss1 (500141) and Mm-

Fos-C2 (316921-C2). Sections were counterstained with DAPI and coverslipped with ProLong Gold (Invitrogen).

Microscopy and Image Analysis

Fluorescent microscopy was performed at the Nikon Imaging Core (UCSD) using a Nikon Eclipse Ti2-E microscope with Plan Apo objectives. Samples were excited by the Lumencor SpectraX and acquired with a DS-Qi2 CMOS camera using NIS-Elements software. Lighting was determined by using the minimum LED intensity and exposure time for each channel using positive and negative control slides, and then used for all subsequent acquisition. Images were imported into FIJI (NIH ImageJ) (43). To determine the number of Kiss1-positive cells in the AVPV, a defined 0.7 mm^2 region encompassing both sides of the third ventricle was set. Kiss1-positive and cFos-positive cells were counted manually, using FIJI Cell Counter tool. Counts were performed by two independent experimenters who were both blinded to genotype.

Puberty, First Estrus, Estrous Cyclicity, and Fertility Assessment

Beginning at weaning (21 days of age), mice were checked daily for pubertal onset. Date of pubertal onset was marked by the occurrence of vaginal opening in females and by preputial separation in males. Following female pubertal onset, vaginal lavages were taken daily until the first occurrence of estrus was observed. Beginning at 12 weeks of age, vaginal smears were taken for 16 consecutive days to assess estrous cyclicity. The slides used for vaginal lavages were stained with 0.1% methylene blue stain and stage of cycle was determined by the composition of cell types present (44). To assess fertility, 12-15-week-old virgin $Vax1^{KissCre}$ or $Vax1^{WT}$ mice were paired with a $Vax1^{WT}$ breeder for 90 days. The number of offspring, latency to first litter, and total number of litters were recorded.

Sperm Motility and Total Sperm Count

Cauda epididymides were dissected and placed in M2 media (Sigma-Aldrich) at room temperature. The right epididymis was cut in half and forceps were used to manually expel sperm into M2 media and left undisturbed for 15 minutes. Motile sperm were counted on a hemocytometer and then placed on a 55ºC heat block for 5 minutes to immobilize all sperm. Following immobilization, all intact sperm cells on the hemocytometer were counted. Motile sperm counts were divided by the total counts and multiplied by 100 to determine the percent motility. The left epididymis was minced, filtered through a 70 µM filter (Falcon), and diluted in water. Using a hemocytometer, all sperm heads were counted to determine total sperm count.

Statistical Analysis

Students t-test, Welch's t-test, one-way ANOVA, and two-way ANOVA were used to determine differences between groups as indicated in the figure legends. For one-way and two-way ANOVA, significant effects were followed by Tukey's Honest Significant Difference test. Graphpad PRISM 9 was used for statistical analysis, with $p<0.05$ indicating significance.

Results

Generation of VAX1$^{Flox/Flox}$:Kiss1^{Cre} mice

The loss of a single allele in *Vax1* heterozygous mice has been shown to increase *Kiss1* mRNA in diestrus females (24). To test the hypothesis that the increase of *Kiss1* is mediated by a direct effect of VAX1 within kisspeptin neurons, we first established whether *Kiss1* and VAX1 were colocalized. Using a newly-available VAX1 monoclonal antibody, we confirmed VAX1 is expressed in the SCN (Fig. 1A), an area of high *Vax1* mRNA expression in adulthood according to the Allen Brain Atlas (http://mouse.brain-map.org) (45) (Fig. 1B). We also detected VAX1 protein in tdTomato-containing neurons from Kiss^{Cre}-tdTomato mice (Fig. 1C), establishing the presence of VAX1 in *Kiss1*-expressing neurons in adulthood. Then, we selectively deleted *Vax1* from *Kiss1*-expressing cells in mice by generating Vax1$^{Flox/Flox}$:Kiss1^{Cre} (Vax1^{KissCre}) and

Vax1$^{Flox/Flox}$:Kiss1^{WT} (Vax1^{WT}) mice (Fig. 1D). Exons 2 and 3 of the *Vax1* gene, containing the homeodomain coding region, are flanked by LoxP sites, allowing for the functional protein to be present in Vax1^{WT} mice and excised in Vax1^{KissCre} mice. We collected genomic DNA and verified that recombination of the *Vax1^{Flox}* allele occurred in tissues known to express *Kiss1*, such as the hypothalamus, pituitary, testis, and ovary (18, 19, 46-48), while recombination was absent from male pituitary and tail (Fig. 1E). There was no recombination detected in any tissues from Vax1^{WT} mice (Fig. 1E), signifying intact *Vax1* expression. These findings indicate the successful recombination of the *Vax1^{Flox}* allele in areas known to express *Kiss1.*

VAX1 regulates Kiss1 and Tac2 mRNA in the ARC of male mice

Using Vax1^{KissCre} mice, we tested whether VAX1 plays a role in regulating *Kiss1* gene expression in ARC kisspeptin neurons *in vivo*. We took micropunches of the ARC from Vax1^{WT} and Vax1^{KissCre} intact male and intact diestrus female mice. We found that *Kiss1* was increased 2-fold in Vax1^{KissCre} male mice compared to Vax1^{WT}, while levels in diestrus female mice were unchanged (Fig. 2A, B). We also measured levels of *Tac2* and *Pdyn*, which are coexpressed with *Kiss1* in approximately 90% of ARC kisspeptin neurons (16). We found that *Tac2* mRNA was increased 1.4-fold in Vax1^{KissCre} males, but unchanged in females (Fig. 2C, D). We found no change in *Pdyn* in mutants of either sex (Fig. 2E, F). We did not identify a sex difference in *Vax1* mRNA expression in the ARC of intact male and intact diestrus-staged or OVX + E2-treated females. However, we did observe a significant reduction of *Vax1* levels in OVX + E2-treated females compared to diestrus-staged females (Fig. 2G). These findings show that *Kiss1* is differentially regulated by VAX1 in males and females *in vivo*.

VAX1 regulates the KISS1 promoter in vitro

We next used a human -1313/+27 *KISS1*-Luciferase reporter (hKiss-Luc) (40), which contains three ATTA sites located at -1211 to -1193, one ATTA site located at -1111 to -1108,

and one ATTA site located at -362 to -359 bp upstream of the *KISS1* transcriptional start site (TSS) (Fig. 3A), to examined whether VAX1 can regulate the kisspeptin promoter *in vitro*. We co-transfected hKiss-Luc with various concentrations of a VAX1 expression vector or an empty vector (EV) control into the immortalized mouse ARC (KTaR-1) kisspeptin cell line (39). We found that overexpression of VAX1 represses hKiss-Luc transcription in KTaR-1 cells in a dose-dependent manner (Fig. 3B). To determine if VAX1 mediated *KISS1* repression through any of the three regions on the promoter that contain ATTA sites, we used site-directed mutagenesis to create cis-mutations at -1211 to -1193 bp (μ-1211-1193), -1111 to -1108 bp (μ-1111-1108), and -362 to -359 bp (μ-362-359) on the hKiss-Luc promoter (3A). We found that VAX1 was not able to significantly repress transcription on μ-1211-1193 and μ-362-359 as compared to the control (hKiss-Luc), while μ-1111-1108 was able to repress transcription to a similar degree as hKiss-Luc (Fig. 3C). These findings indicate that, within immortalized kisspeptin neurons derived from the female ARC, VAX1 acts upon two regions of the *KISS1* promoter to mediate repression and are consistent with the effects seen in the male ARC *in vivo*.

To better understand the differential regulation of *Kiss1* expression observed between males and females *in vivo*, we determined whether sex steroids influence the effects of VAX1 on *KISS1* promoter activity. We co-transfected KTaR-1 cells with 50 ng of VAX1 and 100 ng of androgen receptor (AR) in the presence or absence of 10 μM R1881, a synthetic androgen. We found that the combination of VAX1 overexpression and androgen-containing medium caused a significant reduction in hKiss-Luc transcription compared to VAX1 or R1881 alone, and that there was a significant interaction between VAX1 and R1881 ($p<0.05$) (Fig. 3D). To approximate the female hormonal milieu *in vitro*, we transfected KTaR-1 cells with 50 ng of VAX1 and 50 ng of estrogen receptor alpha (ERα), in the presence or absence of 1 pM E2. We show that E2, along with ERα can repress *hKiss-Luc* transcription (Fig. 3E). We found that in the presence of E2, the effects of VAX1 on the *KISS1* promoter were masked and that the effects of the combination of E2 and VAX1 were not different than the effects of E2 or VAX1 alone. However we did observe a

significant interaction between VAX1 and E2 ($p<0.05$) (Fig. 3E). These findings support our *in vivo* results, in which we saw an upregulation of *Kiss1* following the loss of VAX1 in males, but not in females.

Basal serum gonadotropin levels are not altered by loss of Vax1 from Kiss1 cells

Because we observed that overexpression of VAX1 represses *Kiss1* transcription *in vitro* and the loss of VAX1 *in vivo* led to increased *Kiss1* transcription in males, we next wanted to determine whether the loss of VAX1 *in vivo* led to altered levels of circulating LH and FSH. We found that LH levels in $Vax1^{WT}$ and $Vax1^{KissCre}$ males were not significantly different (Fig. 4A). However, they had significantly different variances (F test, $p = 0.005$). We found that circulating levels of FSH (Fig. 4B) between $Vax1^{WT}$ and $Vax1^{KissCre}$ males were not different. We also detected no change in testosterone levels ($Vax1^{WT}$: T = 318.3 ± 133.1 ng/dL, $Vax1^{KissCre}$: T = 135.3 ± 67.5 ng/dL, N=10-13, $p > 0.05$), but found a significant difference in variance (F test, $p = 0.021$). We found no difference among LH and FSH levels (Fig. 4C, D) or E2 ($Vax1^{WT}$: E2 = 3.2 ± 0.2 pg/mL, $Vax1^{KissCre}$: E2 = 3.3 ± 0.2 pg/mL, N=7-8, $p > 0.05$, level of detection = 3.0 pg/mL, all values below level of detection were set to 3.0 pg/mL) between female $Vax1^{KissCre}$ and $Vax1^{WT}$ mice.

VAX1 regulates Kiss1 in the AVPV of females during induced proestrus

After our data suggested that the effect of VAX1 on *Kiss1* was steroid-dependent in the ARC, we next determined whether VAX1 has a role in the regulation of *Kiss1* in the AVPV of female mice. We transfected immortalized mouse AVPV kisspeptin cells (KTaV-3) (39) with VAX1 and found that overexpression of VAX1 repressed the hKiss-Luc promotor, similar to what was observed in KTaR-1 cells (Fig. 5A). We then measured *Kiss1* mRNA in micropunches of the AVPV from intact diestrus female mice, when E2 and AVPV *Kiss1* levels are low (49, 50). We found no change in AVPV *Kiss1* levels between $Vax1^{WT}$ and $Vax1^{KissCre}$ females, differing from our *in vitro* findings (Fig. 5B).

Next, we examined the role of VAX1 in the AVPV during high E2 conditions. We hypothesized that the loss of a repressive element would lead to higher *Kiss1* expression. We induced an LH surge in Vax1^{WT} and Vax1^{KissCre} mice via ovariectomy (OVX) and implantation of an E2 pellet to mimic proestrus levels of circulating E2. In this model, *Kiss1* mRNA and LH are low in the morning, and high in the evening, at the time of the expected LH surge. We performed qRT-PCR on punches from OVX+E2 treated females harvested in the evening of the induced proestrus. Unexpectedly, we found that AVPV *Kiss1* mRNA was significantly reduced in Vax1^{KissCre} mice compared to Vax1^{WT} mice (Fig. 5C). Because we only observed a difference in *Kiss1* gene regulation in OVX + E2-treated females, we wanted to determine if *Vax1* was regulated by different E2 states. We found that AVPV *Vax1* levels were comparable between diestrus-staged and OVX + E2-treated Vax1^{WT} females, when collected between ZT 4-7. We then assessed circulating LH levels to determine if the changes in *Kiss1* mRNA in the AVPV caused a physiological change in the ability of Vax1^{KissCre} females to induce an LH surge. As expected, AM Vax1^{WT} females maintained low LH levels, while PM Vax1^{WT} females had significantly increased levels of LH (Fig. 5E). Despite having reduced AVPV *Kiss1* levels, the LH levels in PM Vax1^{KissCre} females were not significantly different from PM Vax1^{WT} mice (Fig. 5D). The proportion of Vax1^{WT} (6 out of 8) and Vax1^{KissCre} (7 out of 12) mice meeting the surge criteria was independent of genotype ($\chi^2 = 0.586$, df =1).

To understand the mechanisms enabling Vax1^{KissCre} mice to show an LH surge despite reduced *Kiss1* expression, we performed fluorescent *in situ* hybridization to assess *Kiss1* and *cFos* expression (Fig. 6A). Only mice that met the surge criteria were assayed. We measured the overall number of *Kiss1*-containing neurons, as well as the number of *Kiss1* neurons which colocalized with the immediate early gene *cFos* to assess neural activity. We found fewer *Kiss1*-positive neurons in the AVPV at the time of the induced surge in Vax1^{KissCre} mice compared to Vax1^{WT} mice (Fig. 6B). Despite a reduction in the number of overall AVPV *Kiss1* cells, there was an increase in the percent of kisspeptin neurons that colocalized with *cFos* in Vax1^{KissCre} mice

compared to Vax1^{WT} (Fig. 6C). These findings suggest that, despite having lower *Kiss1* mRNA and fewer overall *Kiss1*-positive cells, Vax1^{KissCre} mice have a larger proportion of activated AVPV kisspeptin neurons during the LH surge, which may compensate and result in surge-level LH concentrations.

VAX1 in Kiss1-expressing cells is not required for reproductive function

To investigate whether deletion of Vax1 within kisspeptin neurons would impact gross reproductive function, we measured several parameters, including pubertal onset, estrous cyclicity, spermatogenesis, and fecundity. We found that female and male Vax1^{KissCre} mice have normal timing of pubertal onset (Fig. 7A, B) and females also have normal timing of first estrus (Vax1^{WT}: 41.6 ± 1.4 days, Vax1^{KissCre}: 42.5 ± 1.3 days, N=11-14, $p > 0.05$), suggesting that *Kiss1*-specific VAX1 does not alter sexual maturation in mice. Weights at pubertal onset were comparable between Vax1^{WT} and Vax1^{KissCre} mice for both females (Vax1^{WT}: 12.24 ± 0.23 g, Vax1^{KissCre}: 12.39 ± 0.26 g) and males (Vax1^{WT}: 14.21 ± 0.28 g, Vax1^{KissCre}: 14.77 ± 0. 35g). We observed no disruptions to estrous cyclicity in Vax1^{KissCre} females as measured by cycle length (Fig. 7C) and time spent in each stage of estrous (Fig. 7D). However, male Vax1^{KissCre} mice have significantly reduced total sperm counts compared to Vax1^{WT} (Fig. 7E), but no difference in sperm motility (Fig. 7F). To measure fecundity, we performed a 120-day fertility assessment, in which we paired Vax1^{KissCre} and Vax1^{WT} mice with a male or female wildtype mouse. We found that both female and male Vax1^{KissCre} mice had comparable number of litters to Vax1^{WT} mice (Fig. 7G) and the time to produce the first litter was not different between groups (Fig. 7H). There were no significant differences in the number of pups born in each litter (Fig. 7I). Given these assessments, we found that the loss of VAX1 from kisspeptin cells does not impact gross fertility measures in either sex.

Discussion

While the importance of kisspeptin signaling within the reproductive axis is unquestioned, the dynamics of *Kiss1* gene regulation are not well established. We previously demonstrated that the heterozygous loss of the homeodomain transcription factor VAX1 leads to increased *Kiss1* expression in the AVPV of female mice (24). Using our $Vax1^{KissCre}$ mouse model and immortalized kisspeptin cell lines, we have established that VAX1 is a regulator of *Kiss1 in vitro* and *in vivo* and this regulation is dependent on brain region and hormone conditions. We found that VAX1 regulates *Kiss1* expression in the male, but not female ARC, and in the female AVPV at the time of the LH surge, but these changes were not sufficient to significantly affect fertility.

$Kiss^{Cre}$-tdTomato mice were utilized to show that adult kisspeptin neurons express VAX1. We then selectively deleted *Vax1* from *Kiss1*-expressing cells by creating $Vax1^{KissCre}$ mice and verified that the *Vax1* allele was recombined in areas that are known to express *Kiss1*. Although *Vax1* was recombined in the female pituitary of the $Vax1^{KissCre}$ mice, it is not expressed in αGSU-expressing cells, such as the gonadotrope cells (31). Correspondence with authors from Ho, et al., 2020, informed us that *Vax1* is mainly constrained to melanotroph cells and was not detected in 8-week-old mouse gonadotropes, according to their single-cell RNA-seq analysis (51). Thus, the recombination detected in the pituitary should not impact gonadotrope function.

The loss of VAX1 alters expression of *Kiss1* and *Tac2*, the gene that encodes for the stimulatory neuropeptide neurokinin B, in the male arcuate. Future studies would be needed to determine if the change in *Tac2* is VAX1-dependent, or a compensatory response to the increase in *Kiss1*. Although we observed increased gene expression of *Kiss1*, we found no significant change in LH and FSH secretion in male $Vax1^{KissCre}$ mice. It is possible that the increase in *Kiss1* was not sufficient to cause a physiologic change in LH secretion. However, while the difference in LH levels was not significantly different in male $Vax1^{KissCre}$ versus $Vax1^{WT}$ mice, we did find a significant difference in the variation between these groups. It is important to note that these LH values were taken from a single time point, and did not evaluate LH pulses. One possibility is that

increased *Kiss1* could increase LH pulse amplitude or pulse frequency, which would lead to a higher probability of detecting a pulse in a one-time measurement. However, profiling LH pulses in intact male mice is difficult due to pulses occurring only once every two to three hours (52). Further exploration is needed to establish whether or not LH profiles are altered; however, our findings suggest any changes are insufficient to affect overall fertility.

We also found that Vax1^{KissCre} males had a reduction in total sperm production, which is consistent with a phenotype observed in *Vax1* heterozygous mice (24). We observed a less severe sperm reduction in Vax1^{KissCre} compared to that reported in the *Vax1* heterozygotes, and we reported no impairments in reproductive capacity in Vax1^{KissCre} males. Several studies have reported that male mice are able to maintain fertility and fecundity despite large reductions in total sperm. For example, *Arl4*-null mice had a 60% reduction and FSH-deficient mice had a 75% reduction in total sperm counts without impairments to litter size or frequency (53, 54). We cannot conclude whether the sperm reduction in our Vax1^{KissCre} mice is due to a loss of *Vax1* in kisspeptin neurons or if it is caused within the testis, as *Vax1* and *Kiss1* both are expressed therein (24). Within the mouse testis, *Kiss1* mRNA and kisspeptin protein have been reported in Leydig cells and elongated spermatids, and may play roles in sperm capacitation and spermatogenesis (47, 55-58). However, it remains to be determined which cell types in the testis express *Vax1* as no *Vax1* enrichment was detected in a microarray analysis from an HA-pulldown from either Leydig cell-specific or Sertoli cell-specific RiboTag mice (59). Sperm production could also be affected by changes to upstream hormone secretion. LH binds to receptors on Leydig cells to promote the synthesis of testosterone, driving spermatogenesis (60, 61). Correct levels of circulating LH are important for maintaining these processes as, in humans, increased LH levels are associated with decreased sperm counts (62, 63). While this association has not been investigated in mice, it leads us to postulate that an increase in LH levels or pulse frequency, driven by increased *Kiss1*, could lead to a reduction in total sperm production.

Using immortalized kisspeptin cell lines, we demonstrate that VAX1 acts as a repressor of the *KISS1* promoter *in vitro*. VAX1 can regulate transcription through binding at ATTA consensus sites (26, 28, 30, 64). The human *KISS1* promoter contains 5 ATTA sites within the 1313 bp upstream of exon 1 (http://genome.ucsc.edu/) (65), presenting potential sites for VAX1 to act as a direct regulator of *KISS1* transcription. Indeed, we found that two regions containing ATTA sites on the *KISS1* promoter regulated VAX1-mediated repression of the promoter. The most distal -1211 to -1193 bp region, containing three ATTA sites, and the most proximal -362 to -359 bp region were both necessary for repression by VAX1. Although homology between the mouse and human *Kiss1/KISS1* promoters is not high (~55% homology according to Needleman-Wunsch alignment between two sequences) (66), the mouse promoter contains 8 ATTA sites within the 1313 bp upstream of the first exon, with multiple regions containing overlapping ATTA sites (http://genome.ucsc.edu/) (65), which could potentially facilitate a similar function.

Intriguingly, we observed that *Kiss1* was differentially regulated by VAX1 in female mice compared to males *in vivo*. We postulate that this sex difference could be due to the interaction of VAX1 with androgens or estrogens. Both androgens and E2 inhibit ARC *Kiss1* mRNA *in vivo* (18, 19) and E2 represses *Kiss1* mRNA in the ARC derived cell line (KTaR-1) *in vitro* (39). We showed, for the first time, that the synthetic androgen, R1881, and E2 can regulate transcription by repressing *KISS1* promoter activity in KTaR-1 cells. Additionally, we observed that the combination of VAX1 and R1881 was able to repress the *KISS1* promoter to a greater degree than either of the two independently, and that there was a significant interaction. The combined effects of VAX1 and E2, on the other hand, could not be differentiated. It is likely that R1881 and E2 are mediating their actions through their steroid receptors, AR and ERα, respectively. It is possible that binding of AR or ERα to the *KISS1* promoter alters VAX1 binding efficiency, or conversely, that binding of VAX1 alters AR or ERα binding. Another possibility is that R1881 or E2 treatments could alter the expression of other genes that are endogenously expressed in the KTaR-1 cell line that could potentially modulate the effects of VAX1. One limitation of the study is

that KTaR-1 cells were derived from a female mouse and the effects of androgens on kisspeptin neurons derived from male ARC could produce a different response (39). Further studies will be required to determine more specifically how steroid hormones acting via nuclear receptors might be interacting with VAX1 on the *KISS1* promoter.

To understand the influence of VAX1 on female AVPV *Kiss1* regulation, we assessed gene expression during diestrus, when we expect AVPV kisspeptin activity to remain low (49), as well as during the preovulatory LH surge, when there is active *Kiss1* mRNA transcription (67). Previously, it was observed that diestrus-staged *Vax1* heterozygous females had elevated AVPV *Kiss1*, serum LH, and E2 levels compared to WT mice. In our study, we found that diestrus Vax1^{KissCre} mice had normal AVPV *Kiss1*, E2, and LH levels. The differences in our data lead us to postulate that the increased AVPV *Kiss1* seen in *Vax1* heterozygotes could be due to positive feedback from the high E2 levels. The source of elevated E2 levels observed in the *Vax1* heterozygous mice is unknown, however, as we did not observe a difference in E2 levels in our Vax1^{KissCre} females, the increase in *Kiss1* in *Vax1* heterozygous mice is likely driven by the loss of *Vax1* from cell populations outside of kisspeptin neurons. *Vax1* heterozygous mice have a copy of *Vax1* deleted from all *Vax1*-expressing cells in the body, including all of those in the hypothalamus, while the homozygous deletion of *Vax1* in Vax1^{KissCre} mice is confined to kisspeptin neurons. The differences in our data could also be due to a developmental effect, resulting from the timing of Kiss1^{Cre} onset of expression. While the *Vax1* haploinsufficiency is present throughout development (68), the Kiss1^{Cre} is not expressed in AVPV kisspeptin neurons until *Kiss1* expression begins postnatally (P10-16) (69), potentially allowing Vax1^{KissCre} females to overcome developmental modulation of the kisspeptin neurons that occurs prior to *Kiss1* expression and thus, VAX1 deletion.

To examine *Kiss1* levels during heightened AVPV kisspeptin activity, we used a validated E2-induced LH surge paradigm (70). The presence of both E2 and a circadian signal is required for the induction of an appropriately timed LH surge. We found that *Kiss1* mRNA levels in

Vax1^{KissCre} mice were significantly lower than Vax1^{WT} mice when collected at the time of lights off. These findings deviate from our *in vitro* findings, and suggest a complex relationship between VAX1, E2, and circadian regulation. Despite changes in *Kiss1* gene expression, Vax1^{KissCre} mice were still capable of inducing an LH surge. Upon closer examination of the molecular changes occurring at the time of the surge, we found that Vax1^{KissCre} females had fewer *Kiss1*-positive cells in the AVPV than Vax1^{WT} mice. We were unable to determine if this reduction was a true reduction in the number of kisspeptin cells, or a reflection of decreased *Kiss1* mRNA that led to fewer cells being detected. Future experiments using lineage tracing will need to be performed to determine if VAX1 is necessary for the development or survival of kisspeptin neurons or for the maintenance of *Kiss1* gene expression in adulthood. Although there was an overall reduction in the number of *Kiss1*-positive cells, there were approximately 10% more *Kiss1*-positive cells that colocalized with *cFos* in Vax1^{KissCre} mice than in Vax1^{WT} mice. This indicates that a higher proportion of Kiss1 neurons are active (*cFos* is expressed in activated neurons), potentially compensating for the overall reduction in *Kiss1* neurons. These findings are consistent with the ability of Vax1^{KissCre} females to produce an LH surge and maintain fertility.

This study shows for the first time that the homeodomain transcription factor VAX1 is a transcriptional repressor of *Kiss1* transcription. We show that VAX1 differentially regulates ARC *Kiss1* expression in males and females *in vivo* and VAX1 differentially regulates the *KISS1* promoter in the presence of androgens and estrogens *in vitro*. We confirmed a previous association between loss of *Vax1* and reduced sperm production, although it is insufficient to alter fecundity. In addition, we found that *Kiss1* mRNA levels and the number of *Kiss1*-expressing neurons in the AVPV were reduced at the time of an E2-induced LH surge. The changes in *Kiss1* expression did not significantly impact fertility, hormone levels, or the ability to mount an LH surge. Overall, these findings increase our understanding of the impacts of homeodomain transcription factors on *Kiss1* gene regulation.

Acknowledgements

We thank Peng Hu for his correspondence regarding their single cell RNA-seq analysis of 8-week old mouse pituitaries. We thank Alejandro Lomniczi and Sergio Ojeda for providing the hKiss-Luc plasmid and Patrick E. Chappell for providing the KTaR-1 and KTaV-3 cell lines. We also thank Jessica S. Lee for her help setting up preliminary experiments and Ichiko Saotome and Austin Chin for technical assistance.

Chapter 1 has been accepted for publication in *Molecular and Cellular Endocrinology*. (Lavalle, Shanna N.; Chou, Teresa; Hernandez, Jacqueline; Naing, Nay Chi P.; Tonsfeldt, Karen J.; Hoffmann, Hanne M; Mellon, Pamela L. 2021. *Kiss1* is differentially regulated in male and female mice by the homeodomain transcription factor VAX1. *Molecular and Cellular Endocrinology* [In Press]). The dissertation author was the primary investigator and author of this paper. Teresa Chou, Jacqueline Hernandez, and Nay Chi Naing provided technical assistance. Karen Tonsfeldt provided technical assistance and assisted with paper composition. Hanne Hoffmann assisted with conceptualization and paper composition. Pamela Mellon supervised the project and provided advice.

Figures

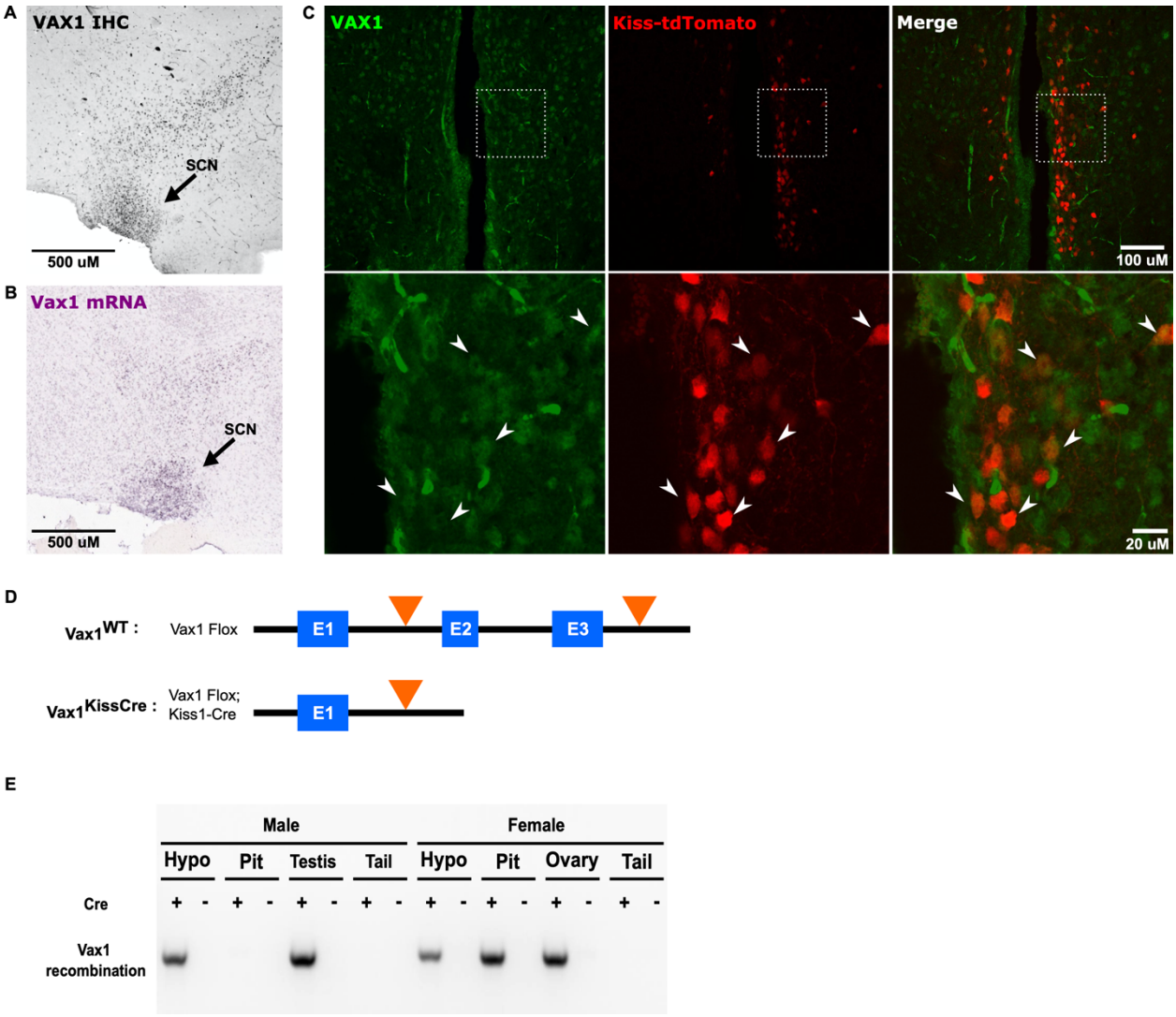

Figure 1.1: VAX1 is expressed in *Kiss1* neurons and recombined in *Kiss1*-Cre-expressing tissues (A) Representative sagittal image of VAX1 immunoreactivity in the suprachiasmatic nucleus (SCN) and surrounding area in an adult WT mouse brain. **(B)** *Vax1 in situ* hybridization from adult male mouse, Allen Brain Atlas, image 18, Vax1 - RP_090303_04_G09 – sagittal, https://mouse.brain-map.org/gene/show/22083. **(C)** Fluorescent imaging showing VAX1 (green) and tdTomato (red) in Kiss1^{Cre}-tdTomato mice. Arrows show colocalization of tdTomato-positive neurons and VAX1. (**D)** Schematic of the *Vax1* gene in Vax1^{WT} and Vax1^{KissCre} mice. Black line depicts intronic sequence, blue boxes represent exons, and orange triangles depict LoxP sites. **(E)** Representative PCR to show recombination of the *Vax1^{Flox}* allele from genomic DNA, collected from tissues known to either express *Kiss1* (hypothalamus, pituitary, testis, ovary) or not express *Kiss1* (tail) in Vax1^{KissCre} (Cre+) and Vax1^{WT} (Cre-) mice.

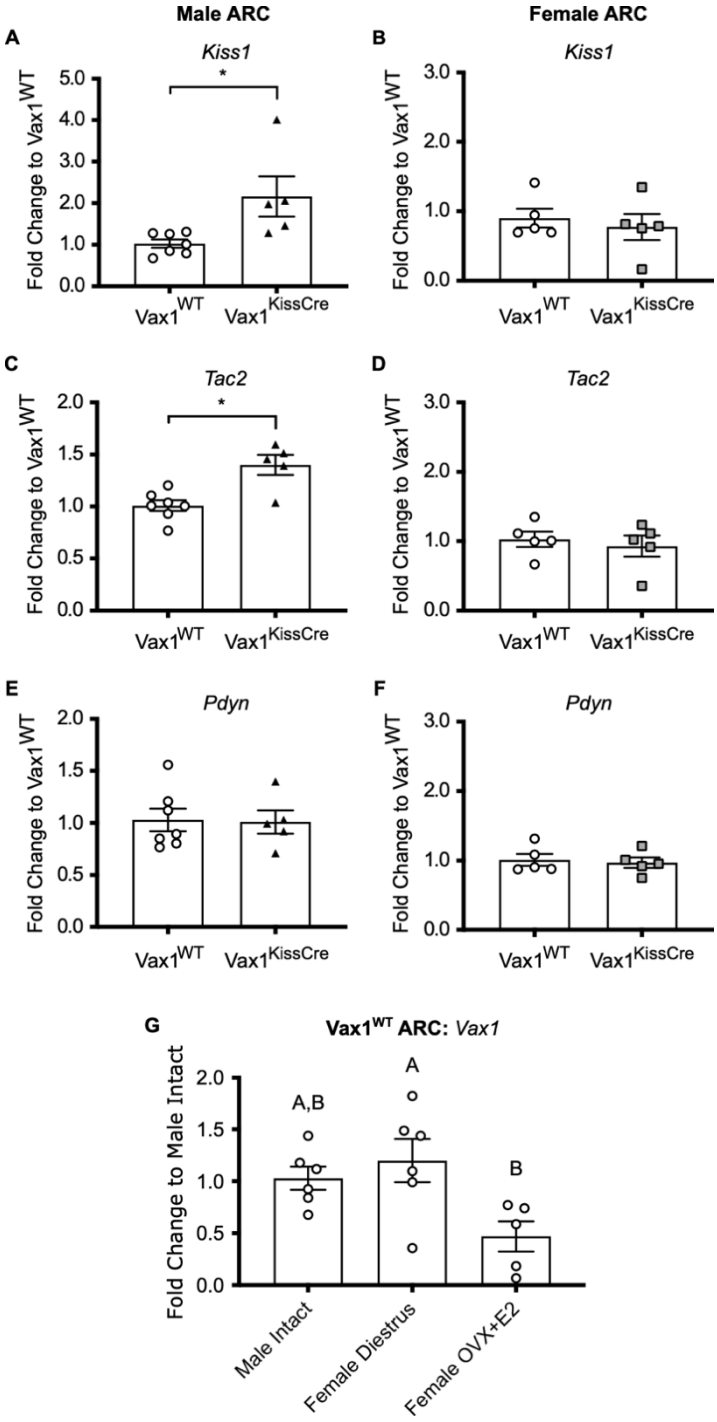

Figure 1.2: VAX1 is required for *Kiss1* and *Tac2* expression in male ARC. RT-qPCR profiles of **(A,B)** Kiss1, **(C,D)** Tac2, and **(E,F)** Pdyn in the ARC of intact males and intact diestrus females. Data were analyzed by the 2^-delta delta Ct method and represented as fold change compared to Vax1WT ± SEM. **(G)** RT-qPCR of Vax1 in ARC of intact Vax1WT males, diestrus-staged Vax1WT females, and OVX+E2 Vax1WT females. Data were analyzed by the 2^-delta delta Ct method and represented as fold change compared to Male Intact ± SEM. All samples were collected between ZT 4-7. All data were analyzed using (A-F) Student's t-test or (G) One-way ANOVA. * or different letters indicate significance of $p<0.05$. N=5-7.

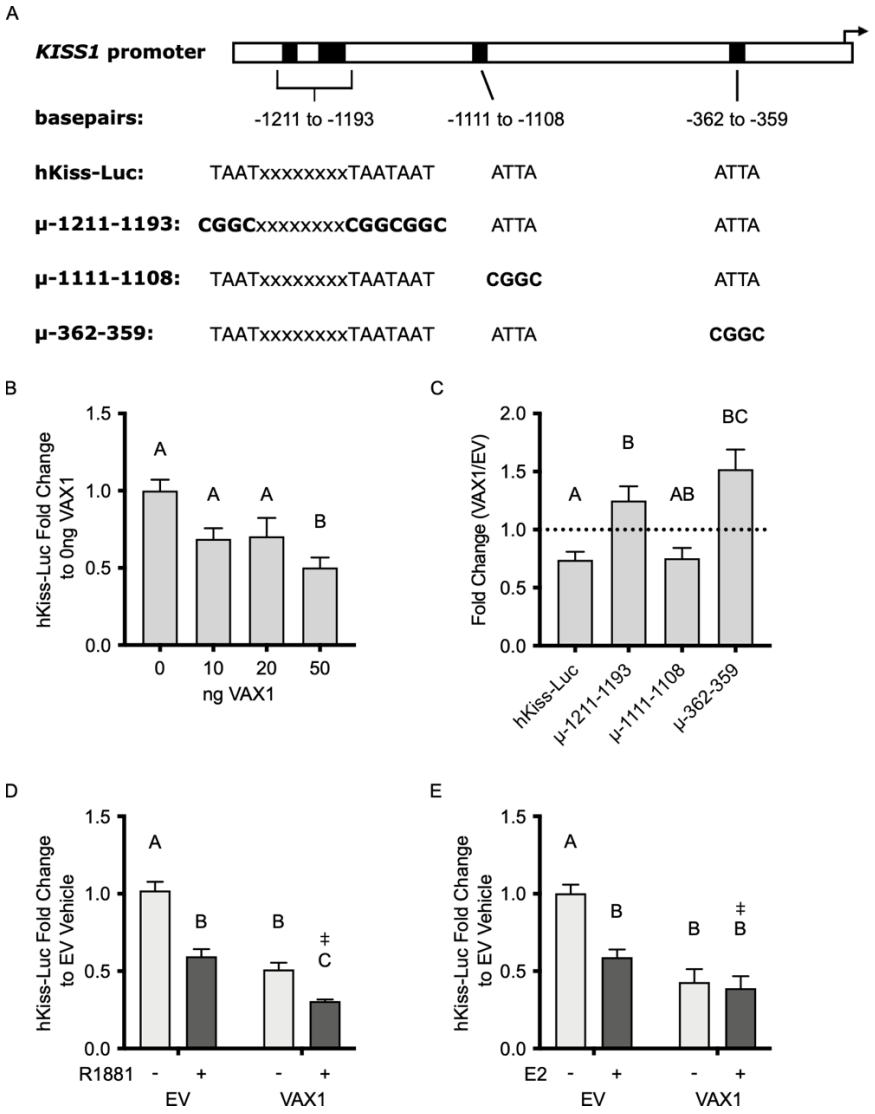

Figure 1.3: VAX1 regulates transcription from the *KISS1* promoter in KTaR-3 cells. (A) Schematic of ATTA binding sites (black rectangles) on the *KISS1* promoter and the sequence of these sites on the hKiss-Luc reporter or hKiss-Luc constructs containing cis-mutations at the indicated positions upstream of the transcriptional start site (black arrow). Bolded sequences indicate base pairs that were changed via site-directed mutagenesis. **(B)** hKiss-Luc was co-transfected with increasing concentrations of VAX1 expression vector into KTaR-1 cells. Data are represented as fold change as compared to 0 ng VAX1. **(C)** hKiss-Luc, μ-1211-1193, μ-1111-1108, and μ-362-359 were co-transfected into KTaR-1 cells with 50 ng VAX1 or EV. Data is represented as fold change of VAX1/EV. Dotted line indicates EV/EV. **(D)** KTaR-1 cells were transfected with hKiss-Luc or pGL2, 50 ng VAX1 or empty vector (EV), and 100 ng AR plasmids, and then treated with 10 μM R1881 (+) or vehicle (-). Data are represented as fold change as compared to EV vehicle. **(E)** KTaR-1 cells were transfected with hKiss-Luc or pGL2, 50 ng VAX1 or EV, and 50 ng ERα plasmids, and then treated with 1 pM E2 (+) or vehicle (-). Data are represented as fold change to EV vehicle. For all experiments, values represent means ± SEM. Data were analyzed using (B, C) One- or (D, E) Two-way ANOVA. Different letters denote significance, $p<0.05$. ‡ denotes a significant two-way factor interaction, $p<0.05$. N=3-4.

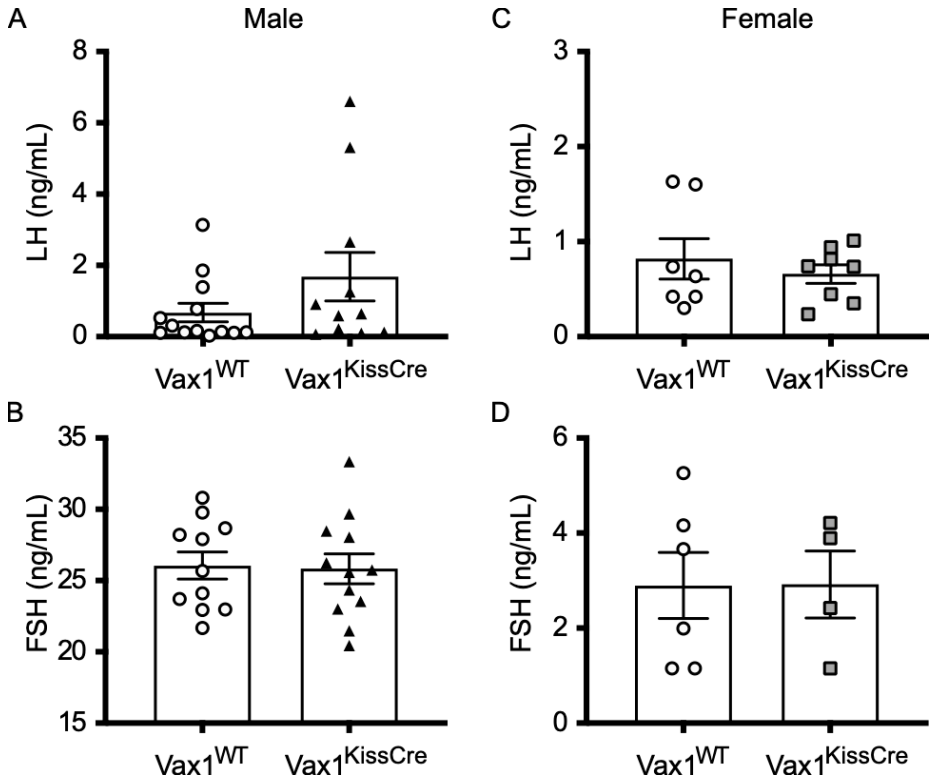

Figure 1.4: Circulating hormone levels are comparable between intact male and female $Vax1^{WT}$ and $Vax1^{KissCre}$ mice. (A) Intact male LH levels. **(B)** Intact male FSH levels. **(C)** Diestrus-staged female LH levels. **(D)** Diestrus-staged female FSH levels. Each symbol represents a biological replicate. Bars represent mean ± SEM. Data were analyzed using (A) Welch's t-test or (B-D) Student's t-test. N=4-7.

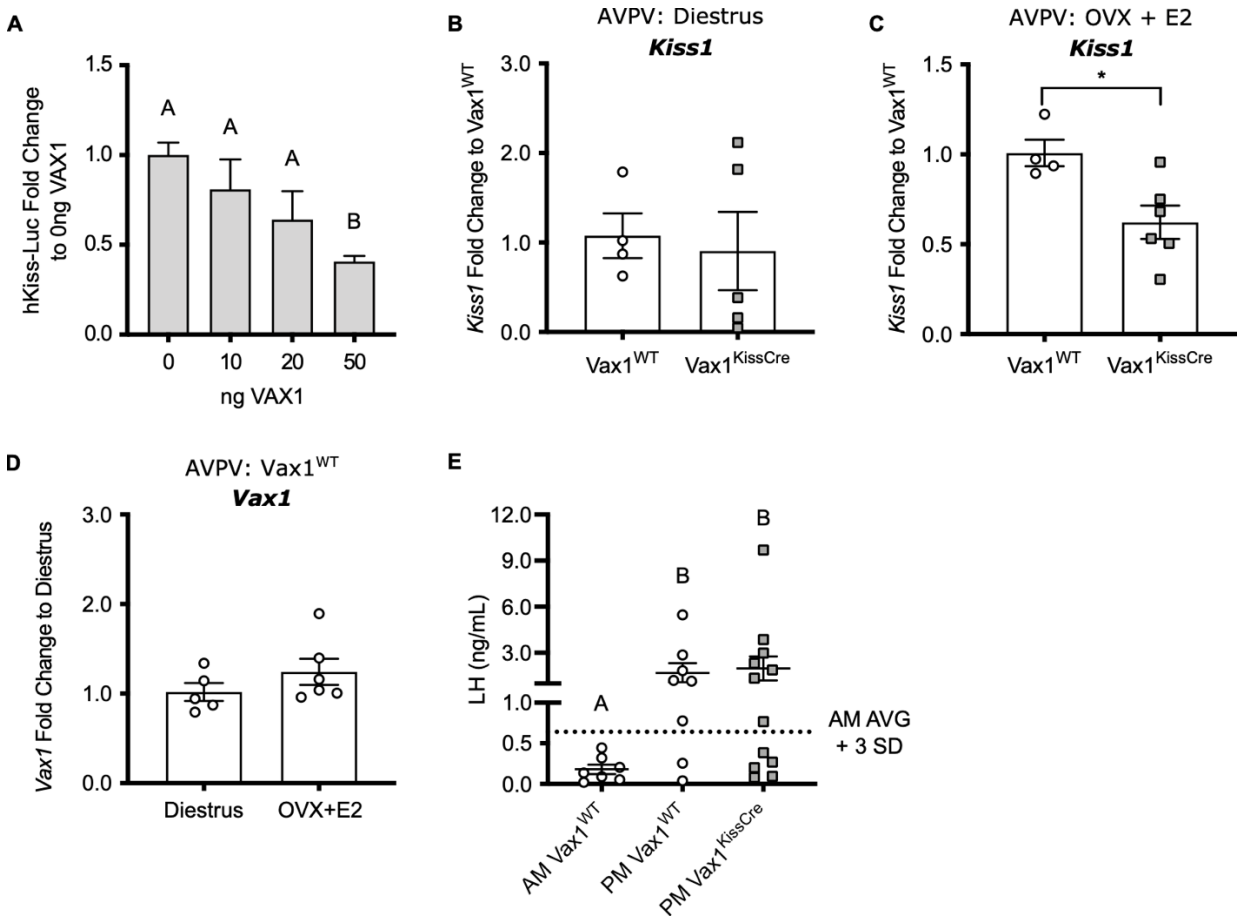

Figure 1.5: *Kiss1* expression is reduced in the AVPV of E2-treated Vax1^{KissCre} females. (A) hKiss-Luc or pGL2 was co-transfected with increasing concentrations of VAX1 expression vector into KTaV-3 cells. hKiss-Luc values were normalized to pGL2 values and represented as fold change compared to 0 ng VAX1. Values represent means ± SEM. N=4. RT-qPCR of *Kiss1* in the AVPV of **(B)** diestrus-staged female mice collected at ZT 4-7 and **(C)** OVX + E2 treated females collected at ZT 12-13. **(D)** RT-qPCR of *Vax1* from the AVPV of intact diestrus-staged Vax1^{WT} collected at ZT 4-7 or OVX + E2-treated Vax1^{WT} females collected at ZT 4-5. qPCR data were analyzed by the 2^-delta delta Ct method and represented as fold change compared to (B, C) Vax1^{WT} or (D) Diestrus ± SEM. (E) Serum LH levels from OVX+E2 treated females, collected at ZT 4-5 (AM) or at ZT 12-13 (PM). Dotted line indicates surge threshold (AM average + 3 SD = 0.64 ng/mL), N=7-12. Data were analyzed using (A, E) One-way ANOVA or (B-D) Student's t-test. Different letters or * indicate significance of $p<0.05$.

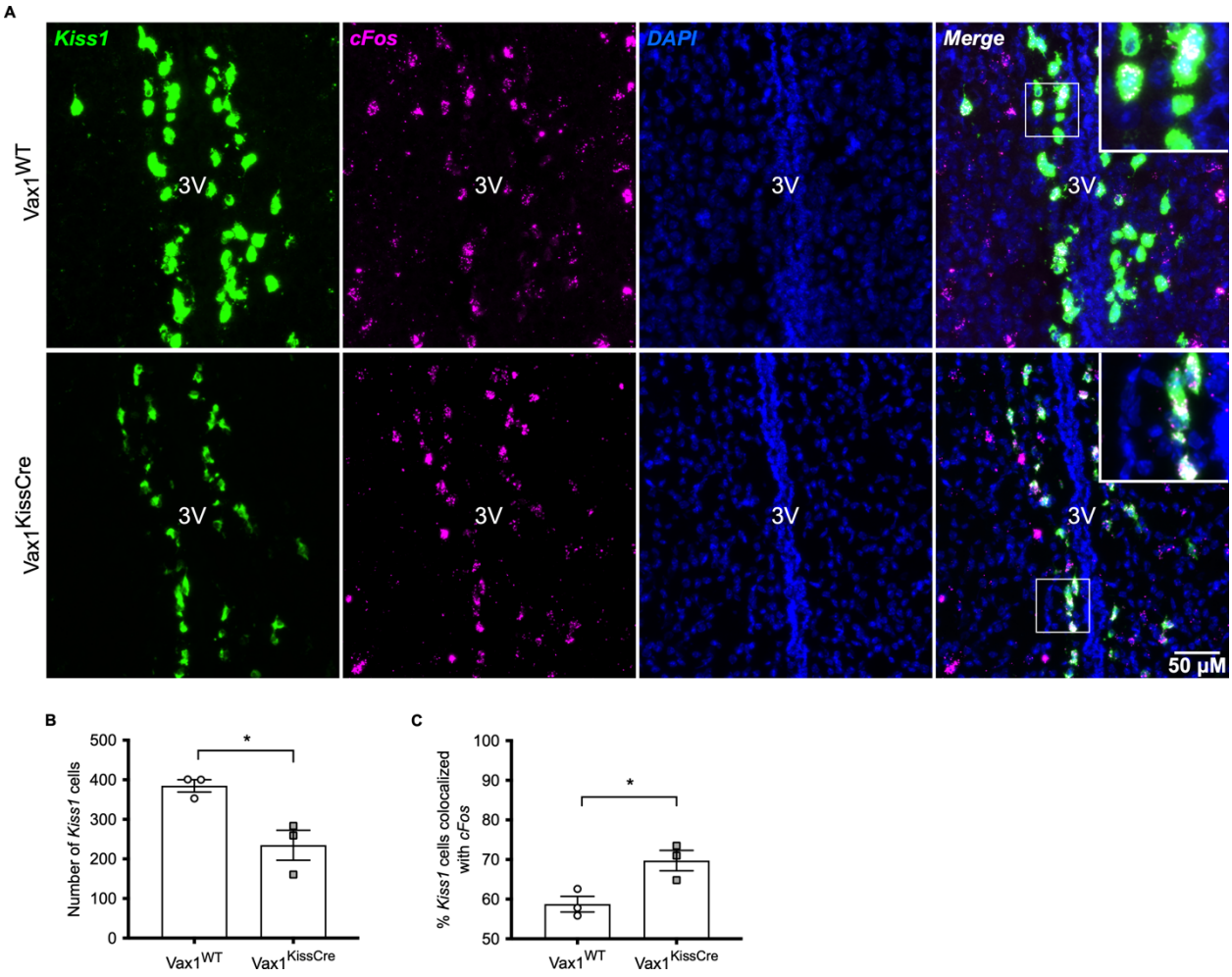

Figure 1.6: Vax1KissCre females have fewer Kiss1 neurons and increased cFos colocalization during an E2-induced LH surge. (A) Representative images of fluorescent *in situ* hybridization to detect *Kiss1* (green) and *cFos* (magenta) in the AVPV of OVX+E2 treated females collected at ZT 12-13. Colocalization of *Kiss1* and *cFos* are visualized in white. Sections were counterstained with DAPI (blue) for visualization of nuclei. **(B)** Quantification of the number of *Kiss1*-positive cells, N=3 per group. **(C)** Percentage of *Kiss1* cells colocalized with *cFos*, N=3 per group. **(B,C)** Data were analyzed using Student's t-test. *, $p<0.05$.

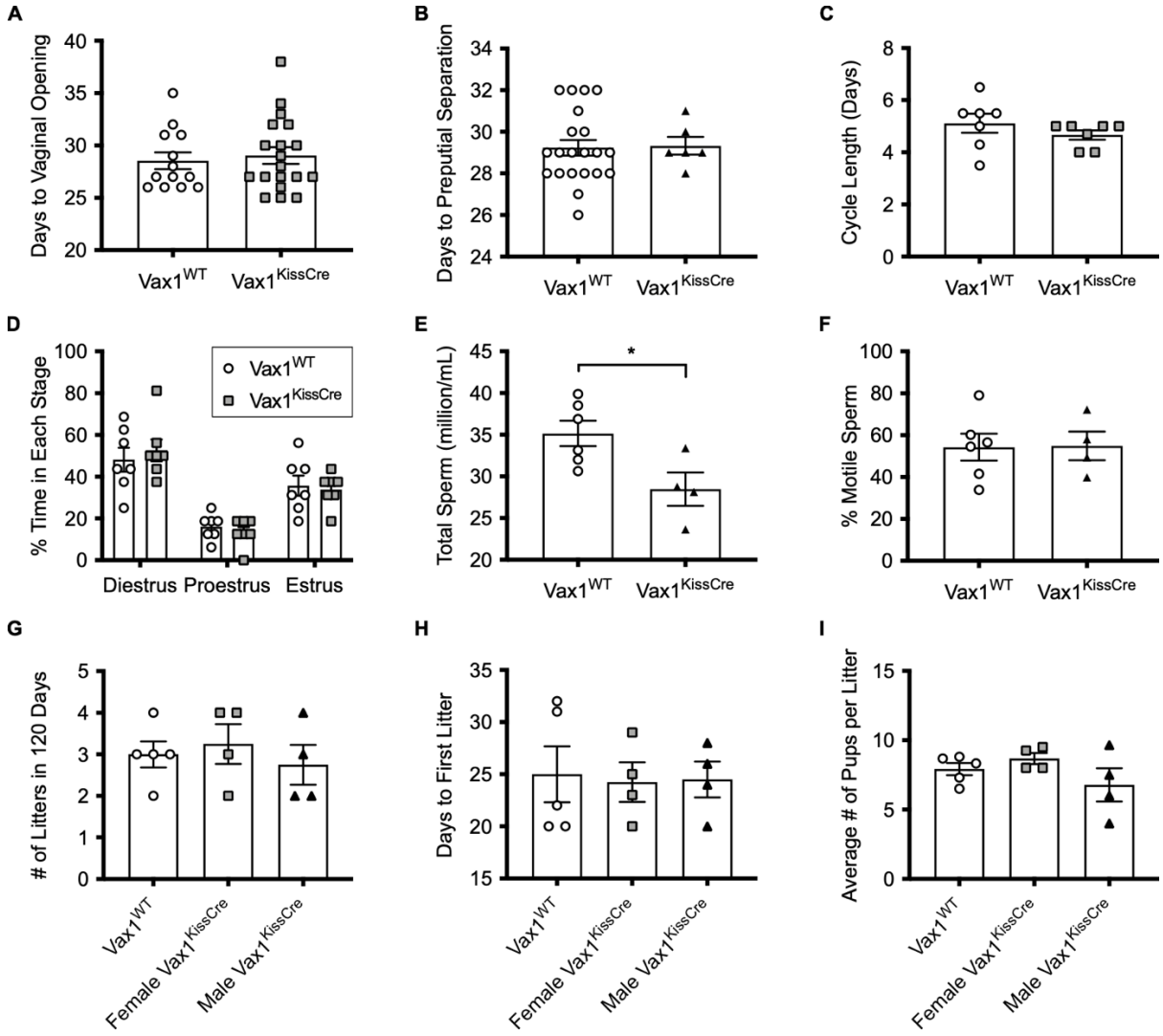

Figure 1.7: Deletion of VAX1 from kisspeptin cells does not alter reproductive function. (A) Time to pubertal onset in females determined by the number of days to reach vaginal opening. N=13-18. **(B)** Time to pubertal onset in males determined by the number of days to preputial separation. N=6-21. (**C)** Time spent in each stage of the estrous cycle within a 16-day period in female mice. N=7. **(D)** Average length in days to complete one estrous cycle in female mice. N=7. **(E)** Percentage of motile sperm. N=4-6. (**F)** Total sperm concentration per epididymis. N=4-6. **(G)** Number of litters produced in 120 days. N=4. **(H)** Number of days until first litter was born. N=4. **(I)** Average number of pups per litter. N=4. For all experiments, values represent means ± SEM. Data were analyzed using One-way ANOVA or Student's t-test. *, $p<0.05$.

Chapter 2: The deletion of the homeodomain gene *Six3* from kisspeptin neurons causes subfertility in female mice

Abstract

The homeodomain transcription factor SIX3 has recently been identified as an important regulator of reproduction, but the cell populations that mediate this role are unknown. The neuropeptide, kisspeptin, is a critical regulator of the reproductive axis and plays roles in sexual maturation, ovulation, and the maintenance of gonadotropin secretion. We selectively deleted *Six3* from kisspeptin neurons in mice to test the hypothesis that kisspeptin-specific SIX3 is required for reproduction. This study establishes a role for SIX3 in kisspeptin neurons in regulating estrous cyclicity and female fertility. We also identified a novel role of SIX3 as a repressor of AVPV *cFos* expression and found that SIX3 in AVPV kisspeptin neurons may play a role in the circadian control of the LH surge.

Introduction

Activation and maintenance of the hypothalamic-pituitary-gonadal (HPG) axis is necessary for the transition from adolescence to adulthood and reproductive competence. Dysregulation along the HPG axis can lead to reduced or complete loss of fertility. Idiopathic hypogonadotropic hypogonadism (IHH) and its anosmic counterpart, Kallmann syndrome, are examples of reproductive disorders that lead to delayed or absent puberty. IHH is a disorder of genetic origin that is characterized by insufficient production or secretion of gonadotropin-releasing hormone (GnRH), leading to low gonadotropin levels, hypogonadism, and a reduction in sex steroids. (11, 71, 72). In humans, mutations in genes critical to kisspeptin signaling, such as *Kiss1* and the *Kiss1r* genes, account for approximately 5% of all normosmic IHH cases (71).

The neuropeptide kisspeptin has established roles in puberty, ovulation, and maintenance of pulsatile GnRH and resulting hormone (LH) secretion in rodents and primates (1, 4, 9). *Kiss1* is differentially regulated in the arcuate nucleus (ARC) and the anteroventral periventricular

nucleus (AVPV) leading to differing roles in reproduction (18, 19). ARC kisspeptin neurons are considered important for the pulse generator and mediate sex steroid negative feedback, leading to reduced *Kiss1* expression in the presence of androgens and estrogens (19, 20, 73). AVPV kisspeptin neurons are sexually dimorphic and primarily occur in females, where they mediate the circadian-gated, estradiol (E2)-induced LH surge and induce *Kiss1* expression in the presence of E2 (18, 21, 22, 74).

Recent studies in mice have implicated homeodomain transcription factors, such as SIX3 and VAX1, as potential IHH gene candidates (23, 24, 27). In mice, deletion of *Vax1* from GnRH neurons results in infertility (30), whereas deletion of *Vax1* from kisspeptin neurons alters *Kiss1* gene expression but does not impact fertility (75). *Six3*, which plays a critical role in eye, nose, and forebrain development (76, 77), is also critical to reproduction in mice. The loss of a single allele results in strong reproductive defects, many of which recapitulate those seen in patients with IHH and Kallmann syndrome, including reduced GnRH neurons in the hypothalamus, altered estrous cyclicity, subfertility, and anosmia (27). However, conditional deletion of *Six3* specifically from GnRH neurons did not recapitulate any of the phenotypes seen in the heterozygous mice, and there were overall no impairments to fertility, suggesting that SIX3 in reproduction occurs in cell populations outside of GnRH neurons (27).

In our current study, we tested the hypothesis that SIX3 in kisspeptin neurons is necessary for fertility by specifically deleting *Six3* from *Kiss1*-expressing cells in mice and found that SIX3 within kisspeptin neurons is necessary for female fertility, but not male, and may play a role in the timing of LH release in the presence of E2.

Methods

Animals

All animal procedures were performed in accordance with the University of California San Diego, Institutional Animal Care and Use Committee regulations. To specifically delete *Six3* from

Kiss1-expressing cells, we crossed $Six3^{flox/flox}$ mice (78, 79) with $Kiss1^{Cre}$ mice (32, 80) to generate $Six3^{Flox/Flox}$:$Kiss1^{Cre}$ mice ($Six3^{KissCre}$) and Six3-flox/flox:$Kiss1^{WT}$ mice ($Six3^{F/F}$). We used Ai9 Rosa-tdTomato mice (33, 81) to create reporter lines by crossing them to $Kiss1^{Cre}$ mice to generate $Kiss1^{Cre}$:tdTomato mice (Kiss1:tdt) and to $Six3^{KissCre}$ mice to generate Six3-flox/flox:$Kiss1^{Cre}$:tdTomato mice (Six3:Kiss1:tdt). All mice were on a mixed NMRI and C57/Bl6 background. Mice were group housed and maintained on a 12-hour light, 12-hour dark cycle with *ad libitum* chow and water.

Genotyping of the mice was performed by PCR with genomic DNA collected from tail tips. *Six3* wildtype (WT) and *Six3* flox alleles were detected using Six3-Forward: 5'-CCCCTAGCCTAACCCAAACAT-3' and Six3-Reverse: 5'-CGGCCCATGTACAACGCGTAT-3' primers. Germline recombination was detected using Six3-Forward and Six3-Rec-Reverse: 5'-TTCCCCTCTTTGACTCCTATG-3' primers. Mice that were positive for *Six3* germline recombination were removed from the study. To identify mice that were Cre-positive, Cre-Forward: 5'-GCATTACCGGTCGTAGCAACGAGTG-3' and Cre-Reverse: 5'-GAACGCTAGAGCCTGTTTTGCACGTTC-3' primers were used. tdTomato was detected using tdtF1: 5'-GGCATTAAAGCAGCGTATCC-3', tdtR1: 5'- CTGTTCCTGTACGGCATGG-3, tdtF2: 5'-CCGAAAATCTGTGGGAAGTC-3', tdtR2: 5'- AAGGGAGCTGCAGTGGAGTA-3.

Immunohistochemistry

Kiss1:tdt and Six3:Kiss1:tdt mice were euthanized at ZT 4-6. Brains were quickly dissected and submerged in 4% PFA overnight. The following day, brains were transferred to 30% sucrose until they sank. 40 µm sections containing the AVPV were sectioned using a cryostat and sections transferred to PBS. On the day of staining, sections underwent heated antigen retrieval in 1X Citra buffer (Biogenex). Sections were washed and underwent blocking for endogenous peroxidases (0.1% H2O2 for 10 m), avidin + 5% normal goat serum block (30 m), and biotin + 5% normal goal serum block (30 m). Slices were incubated overnight in guinea pig

anti SIX3 antibody (82) (Rockland) at 1:1000. The next day, slices were washed and incubated in biotin anti-guinea pig (1:300) for one hour. Slices were washed and then processed with an ABC HRP kit for 30 minutes. Then sections were washed and incubated in 1:250 biotinylated tyramide (Akoya Biosciences) with 0.003% H_2O_2 for ten minutes. Sections were washed again and incubated in 1:200 Streptavidin DyLight 488 (Invitrogen) for 30 minutes. Sections were washed, mounted, and coverslipped with ProLong with DAPI (Invitrogen).

Pubertal onset and estrous cyclicity

After weaning, mice were checked daily for vaginal opening in females and preputial separation in males to determine pubertal onset (83). In females, vaginal smears were taken daily from pubertal onset until first estrus or they reached 90 days of age. To assess estrous cyclicity, vaginal smears were taken for 16 consecutive days from 12-week old females. Vaginal smears were stained with 0.1% methylene blue and an individual, blinded to genotype, determined stage of cell cycle based on the composition of cell types present (44).

Fertility and Plugging Assessment

To assess fertility in females, 15–18-week-old virgin $Six3^{F/F}$ or $Six3^{KissCre}$ females were paired with a virgin wildtype male for 90 days. Mice that exceeded 60 grams in weight were excluded from the study. The number of litters and the number of pups in each litter were recorded. To assess male mating behavior and fertility, 10–16-week-old virgin $Six3^{F/F}$ or $Six3^{KissCre}$ males were paired with a wildtype female for 60 days. For the first 10 days, females were checked for the presence of plugs. The number of pups produced from each litter were recorded.

Ovarian Histology

Following the fertility assay, female mice were separated from males and provided time to birth their final litters, then ovaries were collected during diestrus. Upon dissection, ovaries were

placed in a solution of 60% EtOH, 30% formaldehyde, and 10% glacial acetic acid. Fixed ovaries were paraffin embedded, serial sectioned at 12 μm on a microtome, and stained with hematoxylin and eosin (H&E; Sigma-Aldrich). The number of late antral follicles and the number of corpora lutea within a single ovary was quantified independently by two individuals, blinded to genotype. Every fifth section was scored to ensure follicles and corpora lutea were not double counted.

Hormone Analysis

For diestrus-staged female mice, blood was collected from tail vein via capillary tube (Drummond microcaps 40 μL), sealed with Critoseal, allowed to clot at room temperature for 1 hour, centrifuged at 2000 x g for 15 minutes, and then serum was collected and stored at -20°C until assayed on Luminex Magpix. Serum LH and FSH were measured by Luminex assay according to manufacturer's instructions (LH: lower detection limit, 4.92 pg/mL; intra-assay CV, <14.10%; inter-assay CV 7.28%; FSH: lower detection limit, 9.5 pg/mL; intra-assay CV, 12.13% inter-assay CV 7.22%). For OVX+E2-treated females and intact males, blood samples were collected at time of euthanasia, allowed to clot at room temperature for one hour, centrifuged at 2000 x g for 15 minutes, and then serum was collected and stored at -20°C until assayed. LH and FSH were measured by The University of Virginia Center for Research in Reproduction Ligand Assay and Ansalysis Core. LH was measured using LH RIA with a reportable range between 0.02 – 75.0 ng/mL (intra-assay CV=5.5%, inter-assay CV=8.4%). FSH was measured using FSH RIA with a reportable range between 3.0 – 75.0 ng/mL (intra-assay CV=7.5%, inter-assay CV=10.1%).

Luteinizing hormone (LH) Surge

Between zeitgeiber time (ZT) 2 - 5, 12–16-week-old virgin female mice weighing between 18-28 grams were ovariectomized. A pellet containing 0.75 μg of 17-β estradiol dissolved in sesame oil was implanted subcutaneously to mimic proestrus levels of E2 (21). Two days after

surgery, mice were sacrificed either in the morning (AM), between ZT 4-5, or at the time of lights off (PM), between ZT 12-13. Blood and brains were collected at sacrifice. An LH surge was conservatively defined as LH values that were three standard deviations above the AM average (22).

Fluorescent In-situ Hybridization

20 µm serial coronal sections were collected from fresh frozen brains, spanning the length of the AVPV (34, 84). Sections were mounted on Superfrost Plus Microscope Slides (Fisher Scientific) and stored at -80 until further processing. Slides were fixed in chilled 4% PFA, washed two times with 1X PBS, and dehydrated in ethanol. Probes to detect *Kiss1* (500141), *cFos* (316921-C2), and *Six3* (855211-C3) were used with the RNAscope Multiplex Fluorescent v2 Assay (Advanced Cell Diagnostic, 323100), according to manufacturer's instructions. Sections were counterstained with DAPI and coverslipped with ProLong Gold (Invitrogen). All slides were processed in a single assay.

Microscopy and Analysis

Fluorescent microscopy was performed at the Nikon Imaging Core (UCSD) using a Nikon Eclipse Ti2-E microscope with Plan Apo objectives. Samples were excited by the Lumencor SpectraX and acquired with a DS-Qi2 CMOS camera using NIS-Elements software, or with a laser scanning confocal (A1R HD, Nikon), acquired with an iXon Ultra 897 EMCCD camera (Andor). All slides were imaged at the same time and under the same conditions. Image analysis was performed using NIS-Elements. The NIS-Elements: General Analysis software was used to objectively quantify *Kiss1* intensity, the number of *Kiss1* cells that colocalized with *cFos*, and *cFos* intensity within *Kiss1* cells.

Cell Culture

KTaR-1 (85) and KTaV-3 (86) immortalized kisspeptin cell lines (39) were kindly provided by Dr. Patrick Chappell (Oregon State University). Cells were maintained in complete media consisting of DMEM (Corning) with 10% fetal bovine serum (FBS) (Omega Scientific) and 1% penicillin-streptomycin (HyClone) and incubated at 37°C with 5% CO_2.

Plasmids

The -1313/+26 human *KISS1*-pGL2-luciferase plasmid (hKiss-Luc) (40) was kindly provided by Alejandro Lomniczi and Sergio Ojeda. The -4058/+455 mouse *Kiss1*-pGL4-luciferase plasmid (87) was kindly provided by Dr. Steven Kliewer (UT Southwestern). We subcloned the -4058/+455 mouse *Kiss1* promoter sequence from the pGL4 backbone into a pGL2 backbone using the KpnI-HF, XhoI, and SalI-HF restriction enzymes in 10X Cut Smart Buffer (New England BioLabs) and religated using Quick Ligase Kit (New England BioLabs). This resulted in the -4058/+455 mouse Kiss1-Luciferase-pGL2 plasmid (mKiss-Luc). The murine -1kb cFos-pGL3-Luciferase (cFos-Luc) (88) and the cFos-Luc with cis-mutations at -59 (μ-59), -313 (μ-313), and at both -59 and -313 (μ-313x-59) bp were previously described (89). The reporter plasmid containing β-galactosidase constitutively driven by the Herpes virus thymidine kinase promoter (TK-βgal) was used to control for transfection efficiency. We obtained the SIX3-pSG5 expression plasmid from Origene Technologies (Rockville, MD) and the murine cFOS-CMV expression plasmid (cFOS) was previously described (90). Sequences of all plasmids were confirmed by Sanger Sequencing (Eton Bioscience).

Transient Transfections and Luciferase Assays

One day prior to transient transfections, KTaR-1 or KTaV-3 cells were seeded at 30 x 10^4 cells per well in 12-well plates with complete media and allowed to grow overnight. Transient transfections were performed using Polyjet In Vitro DNA Transfection Reagent (SignaGen Laboratories), following manufacturer's instructions. Cells were transfected with 500 ng of reporter

plasmid (hKiss-Luc, mKiss-Luc, cFos-Luc, μ-313, μ-59, μ-313x-59) or backbone (pGL2 or pGL3), and co-transfected with 100 ng of TK-βgal and 20 ng SIX3 expression vector or pSG5-empty vector (EV) or 50 ng cFOS expression vector or CMV-empty vector (EV). Polyjet/DNA removed 24 hours after transfection treatment and replaced with complete medium. 48 hours from start of transfection, cells were harvested for luciferase assay. To harvest cells, medium was aspirated from wells, cells were washed with 1X PBS, and then lysed with 0.1 M K-phosphate buffer, pH 7.8, containing 0.2% Triton X-100. Luciferase and β-galactosidase assays were performed as previously described. All conditions were performed in triplicate. Within each well, luciferase values were normalized to TK- βgal values, then triplicate luciferase/TK- βgal values were averaged. hKiss-Luc and mKiss-Luc values were normalized to pGL2 and cFos-Luc, μ-313, μ-59, and μ-313x-59 values were normalized to pGL3.

Total Sperm and Sperm Motility

Cauda epididymides were dissected from 12–15-week-old virgin males and placed in room temperature M2 media (Sigma-Aldrich). The left epididymis was minced, filtered through a 70 μM filter, and diluted in water. Sperm heads were counted using a hemocytometer to determine total sperm count. The right epididymis was cut in half and forceps were used to gently expel sperm into M2 media, where they were left undisturbed for 15 minutes. Motile sperm were counted on a hemocytometer and then placed on a heat block for 5 minutes to immobilize all sperm. Following immobilization, all intact sperm cells were counted. Motile sperm counts were divided by intact sperm counts and multiplied by 100 to determine percent motile sperm.

RNA Isolation and qPCR

Brains from 12–15-week-old intact male mice were collected on dry ice and immediately stored at -80°C. Three 250 μm micropunches were collected on a cryostat from the ARC, as previously described (34, 84). RNA from micropunches was isolated with RNeasy Micro Kit

(Qiagen) according to manufacturer's instructions. Purified RNA was converted to cDNA using iScript cDNA Synthesis Kit (Bio-Rad Laboratories), and cDNA products were detected on a Bio-Rad CFX Connect quantitative real-time PCR system (Bio-Rad Laboratories) using SYBR Green Supermix (Bo-Rad Laboratories). Primers to detect *Kiss1*, (Kiss1-Forward: 5'-TGCTGCTTCTCCTCTGT-3', Kiss1-Reverse: 5'-ACCGCGATTCCTTTTGC-3') (37) *Pdyn* (Pdyn-Forward: 5'-GTGTGCAGTGAGGATTCAGG-3', Pdyn-Reverse: 5'-AGTCATCCTTGCCACGGAGC-3') (38), and *Tac2* (Tac2-Forward: 5'-CTGCTTCGGAGACTCTACG-3', Tac2-Reverse: 5'-GGTTGGCTGTTCCTCTTGC-3') (38), were normalized to *Gapdh* (Gapdh-Forward: 5'-TGCACCACCAACTGCTTAG-3', Gapdh-Reverse: 5'-GGATGCAGGGATGATGTTC-3') using the $2^{-\Delta\Delta Ct}$ method (36).

Statistical Analysis

Differences between groups were detected by Student's t-test, Welch's t-test, one-way ANOVA, or two-way ANOVA using Prism 9 (Graphpad). For one-way and two-way ANOVA, significant effects were followed by Tukey's Honest Significant Difference test. Residuals were checked for normality using Shapiro Wilk test ($p<0.05$). When needed, data were log transformed and reanalyzed, where indicated. Significance is indicated by: * $p<0.05$, ** $p<0.005$, *** $p<0.0005$, or by different letters (ANOVA) $p<0.05$.

Results

Deletion of SIX3 in kisspeptin cells disrupts estrous cycles in female mice

To test the hypothesis that SIX3 within kisspeptin neurons regulates reproduction, we specifically deleted *Six3* from *Kiss1* cells by crossing $Six3^{Flox/Flox}$ mice to $Kiss1^{Cre}$ mice to generate $Six3^{Flox/Flox}$:$Kiss1^{Cre}$ mice ($Six3^{KissCre}$) and $Six3^{Flox/Flox}$:$Kiss1^{WT}$ mice ($Six3^{F/F}$). Exon 1 of the *Six3* allele, which contains both the *Six* domain and the homeodomain, is flanked by LoxP sites, allowing this region to be excised from *Kiss1* cells in $Six3^{KissCre}$ mice and remain intact in $Six3^{F/F}$

mice (Fig. 2.1A). Using Kiss1:tdTomato reporter mice (Kiss1:tdt), we demonstrate for the first time that SIX3 is expressed in kisspeptin neurons in mice (Fig. 2.1B). To assess knockdown efficiency, we crossed $Six3^{KissCre}$ mice to Rosa-tdTomato mice to generate $Six3^{Flox/Flox}$:$Kiss1^{Cre}$:tdTomato reporter mice (Six3:Kiss1:tdt) and quantified the number of *Kiss1* cells (detected by tdTomato expression) that were colocalized with SIX3 protein and found that Six3:Kiss1:tdt mice had approximately 16% colocalization, which was significantly lower than the Kiss1:tdt mice that had approximately 56% colocalization (Fig. 2.1C).

We first wanted to test whether the loss of SIX3 from kisspeptin neurons affected sexual maturation in female mice. We found that the loss of *Six3* did not alter the time to pubertal onset, as indicated by vaginal opening (Fig. 2.2A) or the weight at vaginal opening (Fig. 2.2B). The time to reach first estrus, another marker of sexual maturation, was also unaffected (Fig. 2.2C). Female mice have a four to five day estrous cycle in which they transition from diestrus to proestrus and then estrus (44), as shown in representative images of our $Six3^{F/F}$ females (Fig. 2.2D). $Six3^{KissCre}$ females, however, had impaired estrous cycles (Fig. 2.2E). $Six3^{KissCre}$ females spent significantly more time in diestrus and a significantly less time in estrus (Fig. 2.2F), and took approximately twice as long to complete a full cycle (diestrus to diestrus; Fig. 2.2G) compared to $Six3^{F/F}$ females.

Loss of SIX3 from Kiss1-expressing cells reduces fecundity in female mice

Impairments to estrous cyclicity can be an indicator of subfertility, so we then assessed fertility. We paired $Six3^{F/F}$ and $Six3^{KissCre}$ females with a wildtype male breeder for 90 days. We found that there were no significant differences in the number of days to produce their first litter (Fig. 2.3A), or in the total number of litters produced. However, there was a subset of $Six3^{KissCre}$ mice that did not produce a single litter within the 90 days (Fig. 2.3A, B). We also examined litter size and found that $Six3^{KissCre}$ females also had significantly fewer pups per litter compared to $Six3^{F/F}$ females (Fig. 2.3C). To determine if the reduced fecundity was due to an ovulatory defect, we assessed ovarian morphology (Fig. 2.3D). We did not observe any differences in the number

of primary and secondary follicles (data not shown); however, Six3^{KissCre} females had a significant reduction in the number of late stage graafian follicles compared to Six3$^{F/F}$ females (Fig. 2.3E). We found a modest trend towards decreased corpora lutea in Six3^{KissCre} mice (Fig. 2.3F), but the difference was not significant.

Six3^{KissCre} females have elevated LH levels during the morning of induced LH surge

Upon assessment of circulating gonadotropin levels, we found that levels of FSH and LH were similar between diestrus Six3$^{F/F}$ and Six3^{KissCre} females when collected between ZT 4-6 (Fig. 2.4A, B). Because some of the Six3^{KissCre} mice did not produce any litters during the fertility assay (Fig. 2.4A), we assessed their ability to produce an LH surge and found that both PM Six3$^{F/F}$ and PM Six3^{KissCre} females were able to induce an LH surge (Fig. 2.4C). Interestingly, AM Six3^{KissCre} females had significantly elevated levels of LH compared to AM Six3$^{F/F}$ mice (Fig. 2.4C).

To understand what might be driving the elevated LH levels in AM Six3^{KissCre} mice at a molecular level, we collected brains from both AM and PM Six3$^{F/F}$ and Six3^{KissCre} OVX+E2-treated females and visualized AVPV *Kiss1* and *cFos* expression by *in situ* hybridization (Fig. 2.5A). The loss of SIX3 from Six3^{KissCre} mice did not alter the intensity of the *Kiss1* signal in AM or PM females (Fig. 2.5B). The percent of *Kiss1* cells colocalized with *cFos* was significantly higher in the PM group compared to the AM group (Two-way ANOVA, $p<0.05$) and there was a significant reduction in the percent colocalization in AM Six3^{KissCre} mice compared to AM Six3$^{F/F}$ mice (Fig. 2.5C). The intensity of *cFos* was significantly increased in AM Six3^{KissCre} mice compared to AM Six3$^{F/F}$ mice; however, no difference was observed in *cFos* intensity between PM Six3$^{F/F}$ and PM Six3^{KissCre} mice (Fig. 2.5D).

Six3 expression in AVPV kisspeptin neurons is regulated by time of day in the presence of E2

Because we only observed changes in *cFos* colocalization and expression in OVX+E2-treated mice in the AM, we investigated whether *Six3* expression levels were affected by time of

day. We used fluorescent *in situ* hybridization to assess *Six3* expression patters in the AVPV of $Six3^{F/F}$ OVX+E2-treated females (Fig. 2.6A). We found that there was no significant difference in the percentage of *Kiss1* cells that colocalized with *Six3* (Fig. 2.6B). We did observe that *Six3* intensity was significantly lower in the evening (PM), when the LH surge is expected to occur, than in the morning (AM) (Fig. 2.6C), indicating that *Six3* expression in AVPV kisspeptin neurons is regulated by time of day in the presence of E2.

SIX3 represses cFos-Luc transcription in vitro

While the loss of SIX3 from AVPV kisspeptin cells did not alter *Kiss1* mRNA *in vivo*, we wanted test if overexpression of SIX3 could modulate *Kiss1* transcription *in vitro*. We used immortalized kisspeptin cell lines derived from the AVPV (KTaV-3) or ARC (KTaR-1) of a female mouse hypothalamus (39) and cotransfected a human *Kiss1* luciferase (hKiss-Luc) or mouse *Kiss1* luciferase (mKiss-Luc) reporter plasmid with a SIX3 expression vector. We found that overexpression of SIX3 significantly repressed hKiss-Luc transcription in both KTaV-3 (Fig. 2.7A) and KTaR-1 (Fig. 2.7B) cells, but did not alter mKiss-Luc transcription in either cell line (Fig. 2.7C, D). Because we observed altered *cFos* expression in AVPV kisspeptin cells in the morning of an induced LH surge, we wanted to determine if SIX3 could regulate transcription of *cFos*, which has one complete ATTA and a partial (ATTxA) SIX3 binding site located -313 and -59 base pairs upstream of the proximal promoter (Fig. 2.6E). Using a -1 Kb *cFos*-luciferase (cFos-Luc), we demonstrate that SIX3 can act as a repressor of *cFos*-Luc transcription in KTaV-3 cells (Fig. 2.7F). We then tested whether the repression by SIX3 was being mediated through either of the 2 sites. We found that loss of a single ATTA or ATTxA site was not sufficient to prevent SIX3 induced repression of the *cFos* promoters. However, SIX3 could no longer repress cFos-Luc transcription when both of the sites were mutated (Fig. 2.7G). We were also interested in whether cFOS could act as a transcription factor to regulate the *Kiss1* promoter which contains an AP-1 consensus

sequence, a potential binding site for cFOS. We found that overexpression of cFOS significantly induced mKiss-Luc transcription (Fig. 2.7H).

The loss of SIX3 does not impact male fertility

We next examined whether kisspeptin-specific SIX3 is necessary for male fertility. We found that the loss of SIX3 did not alter the length of time to reach puberty, indicated by preputial separation (Fig. 2.7A). The body weight at puberty onset was also similar (Fig. 2.8B). $Six3^{KissCre}$ males had normal sperm production, compared to $Six3^{F/F}$ mice (Fig. 2.8C) but had reduced sperm motility (Fig. 2.8D). $Six3^{KissCre}$ males were able to plug female mice in a similar time frame as $Six3^{F/F}$ males (Fig. 2.8E), and despite reduced sperm motility, produced a similar number of pups per litter (Fig. 2.8F). We found that kisspeptin-specific SIX3 was not needed to regulate circulating FSH (Fig. 2.8G), LH (Fig. 2.8H), or testosterone (Fig. 2.8I) levels. We also examined whether SIX3 could be regulating ARC kisspeptin neuron gene expression. A majority of ARC kisspeptin neurons also secrete the neuropeptides neurokinin B, encoded by *Tac2*, and dynorphin, encoded by *Pdyn*. We took micropunches of the ARC and performed RT-qPCR and found that *Kiss1* (Fig. 2.8J), *Tac2* (Fig. 2.8K), or *Pdyn* (Fig. 2.8L) expression levels were not affected by the loss of SIX3 from male ARC kisspeptin neurons.

Discussion

Heterozygous loss of the homeodomain transcription factor, *Six3*, has previously been shown to cause subfertility in mice (23, 27); however, the specific cell types that mediate this effect are unknown. *Six3* heterozygous mice have functional pituitaries, normal ovarian and testicular morphology, and the homozygous loss of *Six3* from GnRH neurons produced no reproductive impairments (27). We therefore decided to examine the role of *Six3* in kisspeptin neurons, which act upstream of GnRH neurons. We demonstrate for the first time that *Six3* is

expressed in adult kisspeptin neurons in mice and that kisspeptin-specific SIX3 regulates fertility in females.

IHH is characterized by delayed or absent puberty, infertility, and/or low LH and FSH. Kisspeptin signaling has been shown to be a critical component of pubertal onset in both humans and mice (9, 71, 91-93). We found that pubertal maturation was not affected by the loss of kisspeptin-specific SIX3, however, the ability to progress normally through the stages of the estrous cycle was impaired. The increased cycle length in $Six3^{KissCre}$ females was comparable to *Six3* heterozygous females, suggesting that *Six3* in kisspeptin neurons underlies this phenotype (27). This may be due to disruption in sex steroid feedback which is mediated by kisspeptin neurons, and was disrupted on the morning of proestrus (94, 95).

In addition to disrupted estrous cycles, we found that kisspeptin-specific SIX3 is an important regulator of female fertility. We found that the loss of *Six3* from kisspeptin neurons resulted in a subset of $Six3^{KissCre}$ females being unable to produce a single litter within a 90-day fertility assay. The variation in the degree of subfertility observed in $Six3^{KissCre}$ mice could be due to a partially penetrant phenotype or could be due to the efficiency of Kiss1-Cre deletion of *Six3*. Approximately 16% of AVPV kisspeptin neurons retained SIX3 expression in Six3:Kiss1:tdt mice, so it is possible that a more robust phenotype would have been observed if there were a complete knockdown. It is also important to note that SIX3 and SIX6 have a high degree of homology (96) and it is possible that the SIX3 antibody used could also detect SIX6 which would not have been deleted from kisspeptin neurons. The $Six3^{KissCre}$ females that were able to produce litters had reduced fecundity compared to $Six3^{F/F}$ females, which was a more robust reproductive effect compared to *Six3* heterozygous females who had a delay to first litter, but normal fecundity (27). The decreased fecundity is likely due to an impairment in follicular maturation or survival as there were significantly fewer Graafian follicles in $Six3^{KissCre}$ mice. Because *Six3* is not detected in the ovary (97), we speculate that the reduction in late-stage follicles is driven by the loss of SIX3 in kisspeptin neurons.

The variation in the degree of subfertility observed in Six3^{KissCre} mice could be due to a partially penetrant phenotype or could be due to the efficiency of Kiss1-Cre deletion of *Six3*. Approximately 16% of AVPV kisspeptin neurons retained SIX3 expression in Six3:Kiss1:tdt mice, so it is possible that a more robust phenotype would have been observed if there were a complete knockdown. It is also important to note that SIX3 and SIX6 have a high degree of homology (96) and it is possible that the SIX3 antibody used could also detect SIX6 which would not have been deleted from kisspeptin neurons.

Successful ovulation is prompted by the circadian-gated LH surge that occurs on the evening of proestrus (67, 98). We found that Six3^{KissCre} females were able to generate an induced LH surge and that the loss of SIX3 did not alter *Kiss1* levels, *cFos* levels, or *Kiss1-cFos* colocalization at the time of the LH surge. Although there were two Six3^{KissCre} mice that failed to induce a surge, it is likely due to the sensitivity of the LH surge paradigm (21, 70). These findings suggest that these mice can appropriately respond to the cues needed to induce ovulation in the presence of exogenous estrogen. The presence of corpora lutea in intact females that underwent a fertility assay, also supports the finding that Six3^{KissCre} mice are capable of ovulating.

Six3^{KissCre} females had elevated LH serum levels in the morning of an E2-induced LH surge, when kisspeptin neuron activity and LH levels are expected to remain low (49, 50). This finding suggests an impairment in negative feedback, which is regulated by ARC kisspeptin neurons, however, male and diestrus female Six3^{KissCre} mice had normal circulating LH and FSH levels, suggesting negative feedback is intact during low sex steroid states. We next explored whether the cause of the elevated morning LH could be increased or mis-timed kisspeptin secretion from AVPV kisspeptin neurons. We did not observe alterations in AVPV *Kiss1* gene expression in the morning of an induced LH surge, suggesting that the increase is unrelated to *Kiss1* expression in the morning. The immediate early gene (IEG), *cFos*, is a useful marker of neuronal activity as *cFos* expression is induced following neural activity (99, 100). We observed a 10% reduction in the percent of *Kiss1* cells colocalized with *cFos* in AM Six3^{KissCre} mice, which

suggests that AM LH levels are not elevated due to increased neuron activity. Although we observed a reduction in *Six3* colocalization, we found an increase in *cFos* expression, leading us to postulate that SIX3 could indirectly mediate kisspeptin secretion through repression of *cFos*.

cFOS is a pleiotropic transcription factor that can form heterodimers with other IEGs to form the AP-1 transcription factor complex, which can then regulate gene expression (101, 102). Homeodomain transcription factors can interact with IEGs, such as cJUN and cFOS, to regulate IEG gene expression (89, 103). The murine *cFos* proximal promoter contains both a complete (-313 bp) and partial (-59 bp) SIX3 consensus sequence (89) and we show here that SIX3 can act through either of these sites to repress *cFos*-Luc transcription in AVPV kisspeptin neurons *in vitro* and that the loss of SIX3 from kisspeptin neurons *in vivo* leads to increased *cFos* expression on the morning of an E2-induced LH surge. Studies have indicated a possible role of cFOS as a potential regulator *Kiss1* gene expression, as *cFOS*-null mice have an 80% reduction in AVPV *Kiss1* mRNA per cell (104), however, a direct relationship between the two has not been established. The mouse *Kiss1* promoter contains an AP-1 consensus site, which cFOS could potentially bind, and we demonstrate for the first time that cFOS induces the *Kiss1* promoter *in vitro*. Although the effect was modest, cFOS acts as a heterodimer to form the AP-1 transcription factor complex, so it is possible that the presence of other IEGs would elicit a more robust response (103, 105, 106). Although we observed elevated LH levels in AM Six3^{KissCre} females, we did not observe changes in AM AVPV *Kiss1* expression *in vivo*. However, only 30% of *Kiss1* cells expressed *cFos* in the AM, which could make it difficult to detect *cFos*-induced changes in total *Kiss1* mRNA levels. Kisspeptin is a potent stimulator of the reproductive axis, and increased kisspeptin secretion from a small number of kisspeptin neurons could be sufficient to induce the modest elevation in LH that we observed in the AM in Six3^{KissCre} females.

It is also possible that the effects of SIX3 on *cFos* expression are unrelated to the increased LH levels and that SIX3 has a role in regulating the circadian cues that regulate the timing of LH release in the presence of E2. AVPV kisspeptin neurons integrate signals from the

suprachiasmatic nucleus (SCN) to regulate the timing of the LH surge (70, 107, 108). A recent study, which deleted *Six3* from mature neurons using Synapsin-Cre, revealed that SIX3 is important for proper alignment of circadian rhythms and is associated with mistimed *Per2:Luc* expression (109). In the present study, we found that *Six3* expression in AVPV kisspeptin neurons is regulated by time of day in the presence of E2, presenting a potential role in the timing of the LH surge.

We found that SIX3 differentially regulates the human and mouse kisspeptin promoters *in vitro*, by acting as a repressor of hKiss-Luc transcription and having no effect on mKiss-Luc transcription in either ARC or AVPV kisspeptin cell lines. SIX3 is highly conserved with the amino acid sequence being identical between mouse and human (96), suggesting that the contrast is due to differences in the human and mouse promoters. SIX3 regulates transcription through binding of ATTA and ATTA-like motifs (110, 111). While both the human and mouse *KISS1/Kiss1* promoters contain several ATTA sites, the positions of the motifs are not conserved (http://genome.ucsc.edu/) (65). Consistent with what was observed *in vitro*, the loss of SIX3 from kisspeptin neurons in OVX+E2-treated females did not change *Kiss1* mean intensity in either the morning (AM) or evening (PM) of an induced LH surge compared to $Six3^{F/F}$ females.

In addition to the reproductive assessments performed in female mice, we also investigated whether kisspeptin-specific SIX3 was necessary for male fertility. We found that the loss of SIX3 from kisspeptin cells resulted in a 28% reduction in motile sperm; however, there were no impairments to total sperm production, time to plug, or the number of pups per litter. *Kiss1*, *Tac2*, and *Pdyn* gene expression, circulating gonadotropin levels, and testosterone levels were not affected by the loss of SIX3 in males. From these data, we can infer that the reproductive phenotypes observed in the *Six3* heterozygous males were not due to kisspeptin-specific SIX3 populations. This is consistent with previous studies that found the reduced fertility in *Six3* heterozygous males is mainly attributed to abnormal olfaction (27).

Overall, our study establishes the importance of kisspeptin-specific SIX3 in regulating estrous cycles and fertility in female mice. We also demonstrate that *Six3* is regulated by time of day in AVPV kisspeptin neurons and may play a role in the circadian control of the LH surge, through repression of *cFos* within kisspeptin neurons. The impact of SIX3 in human reproduction is yet to be illuminated, but our data demonstrate that SIX3 regulates the human *KISS1* promoter, while it had no effect on the mouse *Kiss1* promoter.

Acknowledgements

We thank Alejandro Lomniczi and Sergio Ojeda for providing the hKiss-Luc plasmid, Steven Kliewer for providing the mKiss-Luc plasmid, and Patrick E. Chappell for providing the KTaR-1 and KTaV-3 cell lines. We also thank Ichiko Saotome and Austin Chin for technical assistance and Daphne Binds and the Nikon Imaging Core for developing the analysis pipeline to quantify our RNAscope images.

Chapter 2 has been submitted for publication to *Endocrinology*. (Lavalle, Shanna N.; Chou, Teresa; Hernandez, Jacqueline; Naing, Nay Chi P.; He, Michelle Y.; Tonsfeldt, Karen J.; Mellon, Pamela L. Deletion of the homeodomain gene *Six3* from kisspeptin neurons causes subfertility in female mice). The dissertation author was the primary investigator and will be the author of this paper. Teresa Chou, Jacqueline Hernandez, Nay Chi Naing, and Michelle He provided technical assistance. Karen Tonsfeldt provided technical assistance and assisted with paper composition. Pamela Mellon supervised the project and provided advice.

Figures

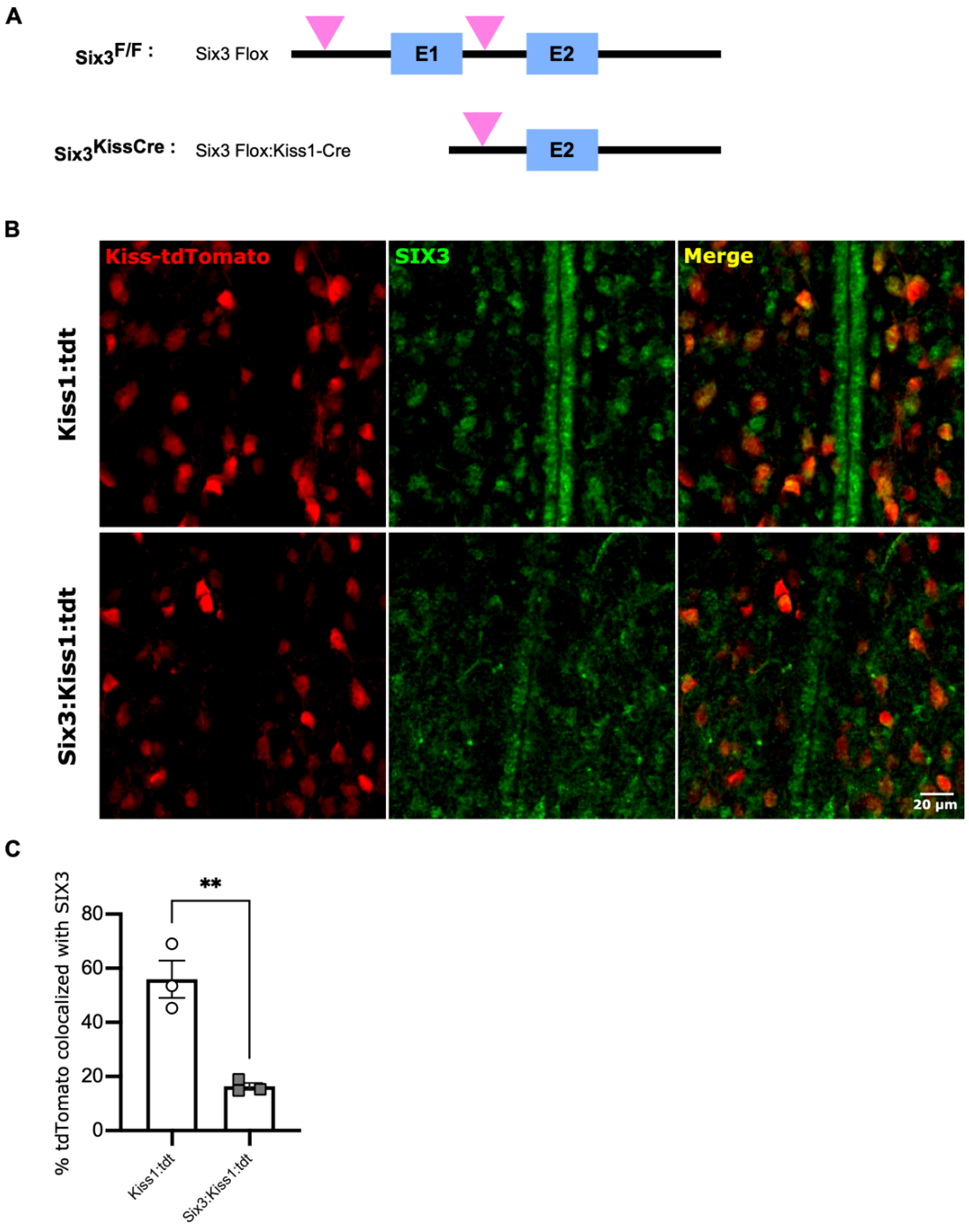

Figure 2.1: SIX3 is expressed in AVPV kisspeptin neurons in mice. (A) Schematic of the *Six3* gene in $Six3^{F/F}$ and $Six3^{KissCre}$ mice. Triangles represent LoxP sites. Blue rectangles represent exon 1 (E1) and exon 2 (E2). (**B)** Fluorescent images of tdTomato (red) and SIX3 (green) protein expression in AVPV kisspeptin neurons in female Kiss1:tdt and Six3:Kiss1:tdt mice. **(C)** Percent of tdTomato cells colocalized with SIX3. Data analyzed by Student's t-test.

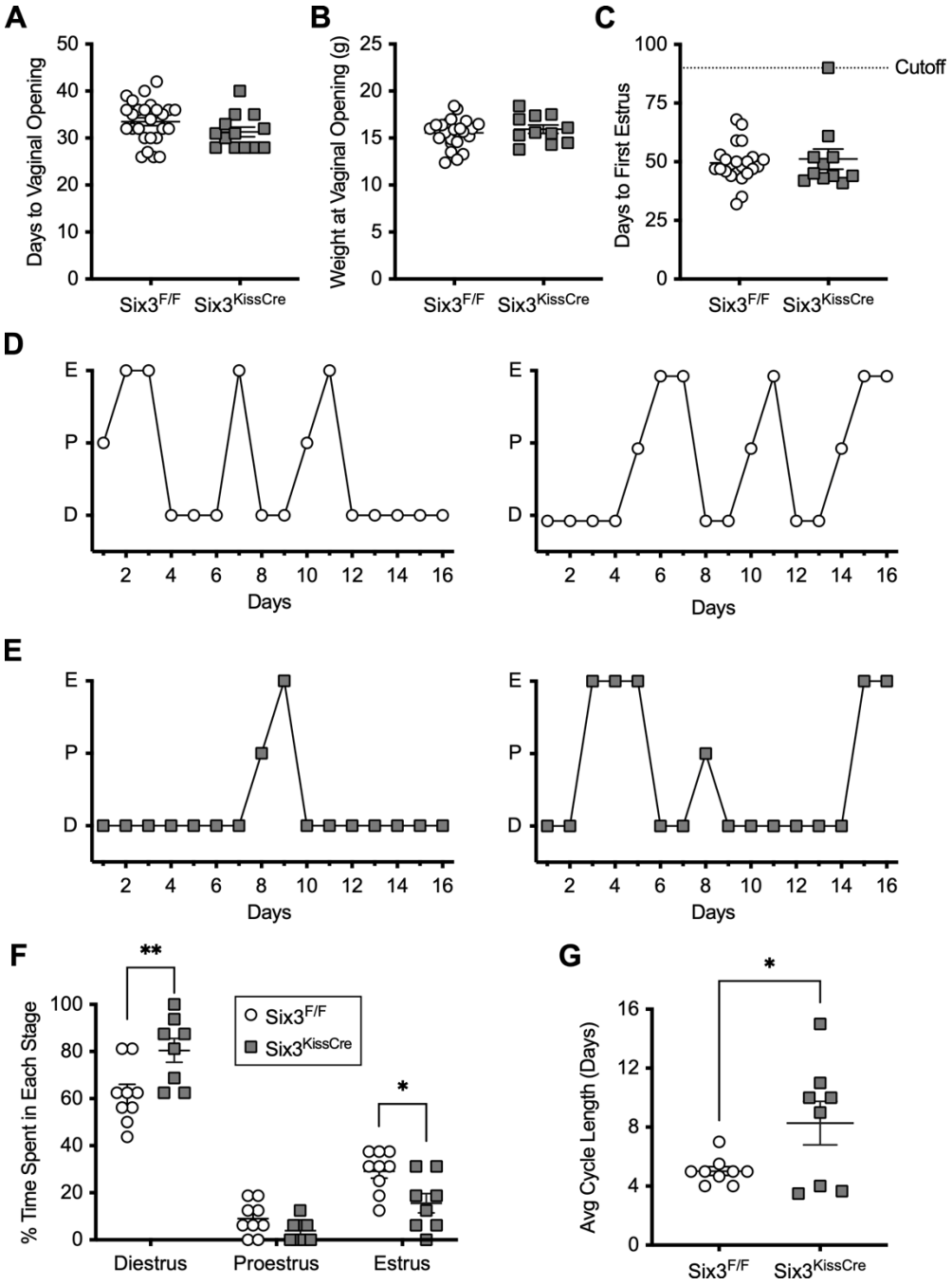

Figure 2.2: Loss of SIX3 from kisspeptin neurons disrupts estrous cyclicity. **(A)** Time to pubertal onset determined by vaginal opening. **(B)** Weight of mice the day of vaginal opening. **(C)** Time to first estrus stage. Representative cycles from **(D)** two $Six3^{F/F}$ females and **(E)** two $Six3^{KissCre}$ females. D indicates diestrus, P indicates proestrus, and E indicates estrus. **(F)** Percent of time spent in each stage of estrous cycle. White circles represent $Six3^{F/F}$ mice and Grey squares represent $Six3^{KissCre}$ mice. **(G)** Average time to complete one estrous cycle, measured from diestrus to diestrus. Data were analyzed by two-way ANOVA or Student's t-test.

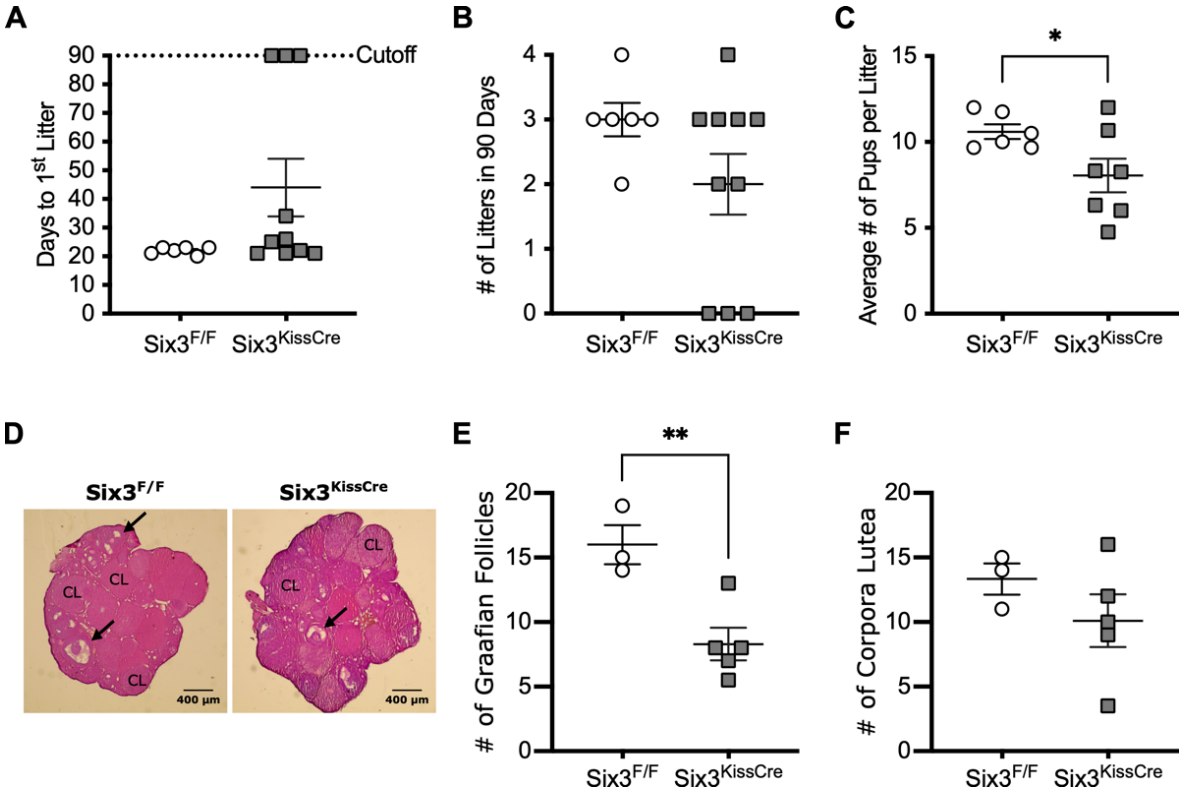

Figure 2.3: *Six3* within kisspeptin cells is necessary for female fecundity. (A) Number of days between pairing and first litter. Dotted line indicates a 90-day cutoff. **(B)** Number of litters produced in 90 days. **(C)** Average number of pups born per litter. **(D)** Representative images of ovaries from $Six3^{F/F}$ and $Six3^{KissCre}$ females collected after fertility assay. Arrows depict examples of Graafian follicles, CL depicts examples of corpora lutea. **(E)** Quantification of the number of Graafian follicles per ovary. **(F)** Quantification of the number of corpora lutea per ovary. All data were analyzed by Student's t-test or Welch's t-test.

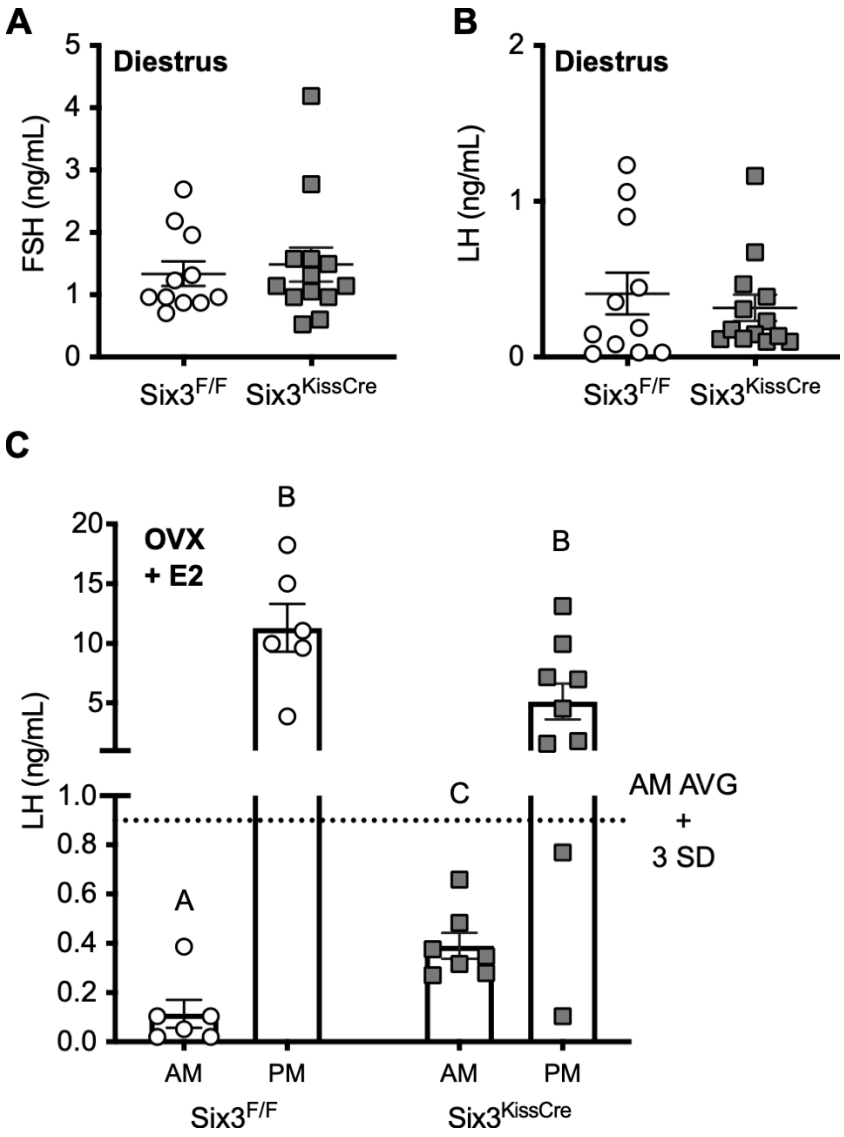

Figure 2.4: Serum gonadotropins in female mice. Circulating serum levels of **(A)** FSH and **(B)** LH in diestrus-staged female mice collected between ZT 4-6. Data were analyzed by Student's t-test. **(C)** Serum LH levels in OVX + E2 treated mice collected at ZT 4-5 (AM) or ZT 12-13 (PM). Dotted line indicates surge threshold (combined AM average + 3 SD = 0.9 ng/mL). Data were log transformed prior to analysis by two-way ANOVA.

Figure 2.5: The loss of SIX3 from kisspeptin neurons reduces the percent of *Kiss1* cells colocalized with *cFos*. (A). Representative images of fluorescent *in situ* hybridization to detect *Kiss1* (Green), *cFos* (magenta) in the AVPV of OVX+E2 treated females collected at ZT 4-5 (AM) or ZT 12-13 (PM). *Kiss1* and *cFos* colocalization are visualized in white. Arrows depict examples of *Kiss1*-*cFos* colocalization. Sections were counterstained with DAPI (blue) for visualization of the nuclei. **(B)** Mean intensity of *Kiss1* in arbitrary units (A.U.). **(C)** Percent of *Kiss1*-cells colocalized with *cFos*. **(D)** Mean intensity of *cFos* within *Kiss1*-positive cells. * represents significance by Student's t-test between indicated pairs

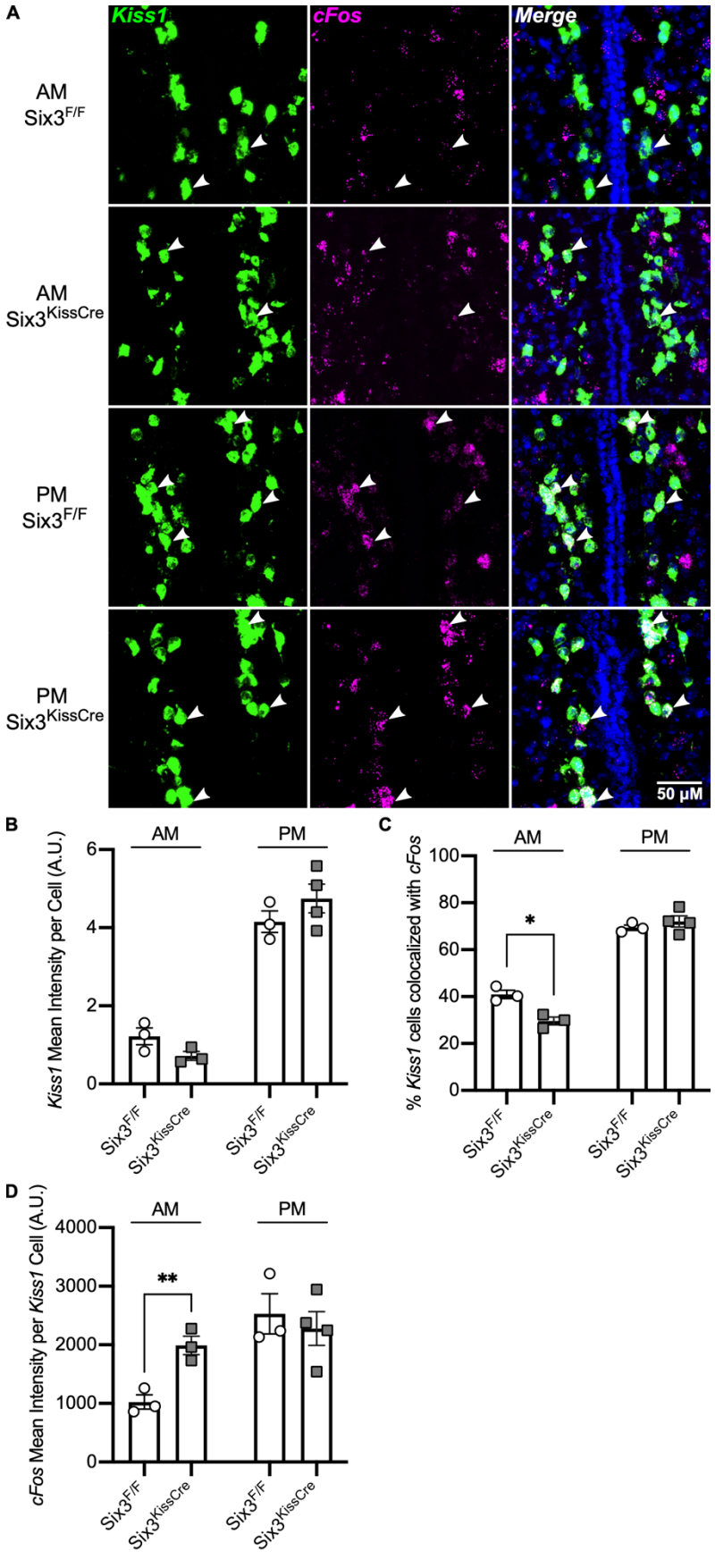
A
Kiss1
cFos
Merge
AM Six3F/F
AM Six3KissCre
PM Six3F/F
PM Six3KissCre
50 µM
B
Kiss1 Mean Intensity per Cell (A.U.)
AM
PM
Six3F/F
Six3KissCre
C
% Kiss1 cells colocalized with cFos
*
D
cFos Mean Intensity per Kiss1 Cell (A.U.)
**

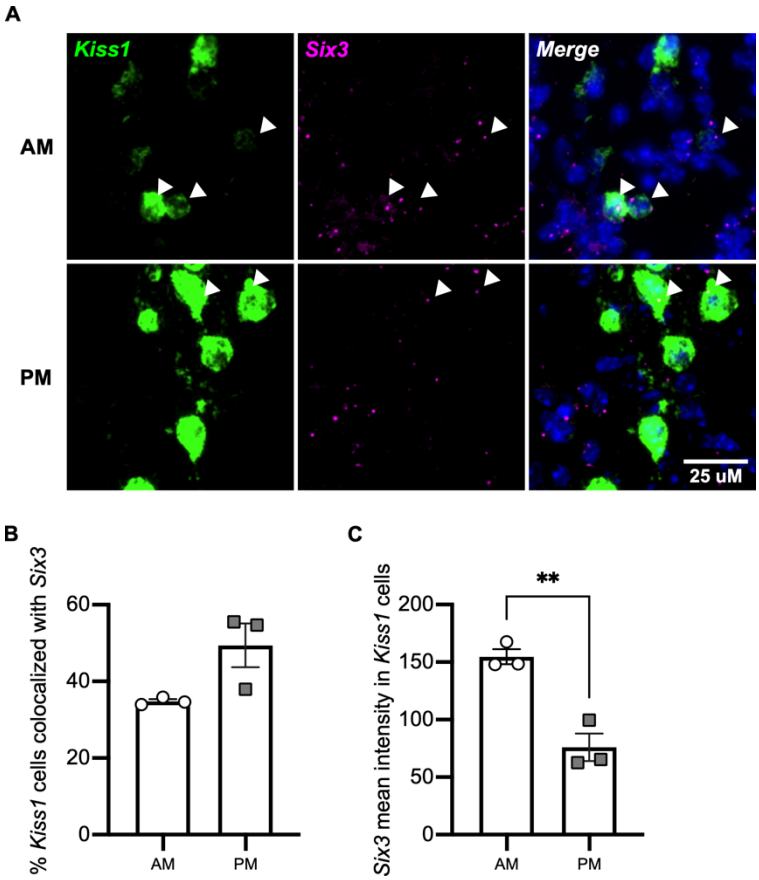

Figure 2.6: *Six3* intensity is regulated by time of day in OVX+E2-treated Six3^{WT} mice. (A) Representative images of fluorescent *in situ* hybridization to detect *Kiss1* (Green) and *Six3* (magenta) in the AVPV of OVX+E2 treated females collected at ZT 4-5 (AM) or ZT 12-13 (PM). Sections were counterstained with DAPI (blue) to visual nuclei. White triangles depict examples of *Kiss1* and *Six3* colocalization. **(B)** Quantification of the percent of *Kiss1* cells colocalized with *Six3*. **(C)** Quantification of *Six3* mean intensity within *Kiss1*-positive cells. Data were analyzed by student's t-test.

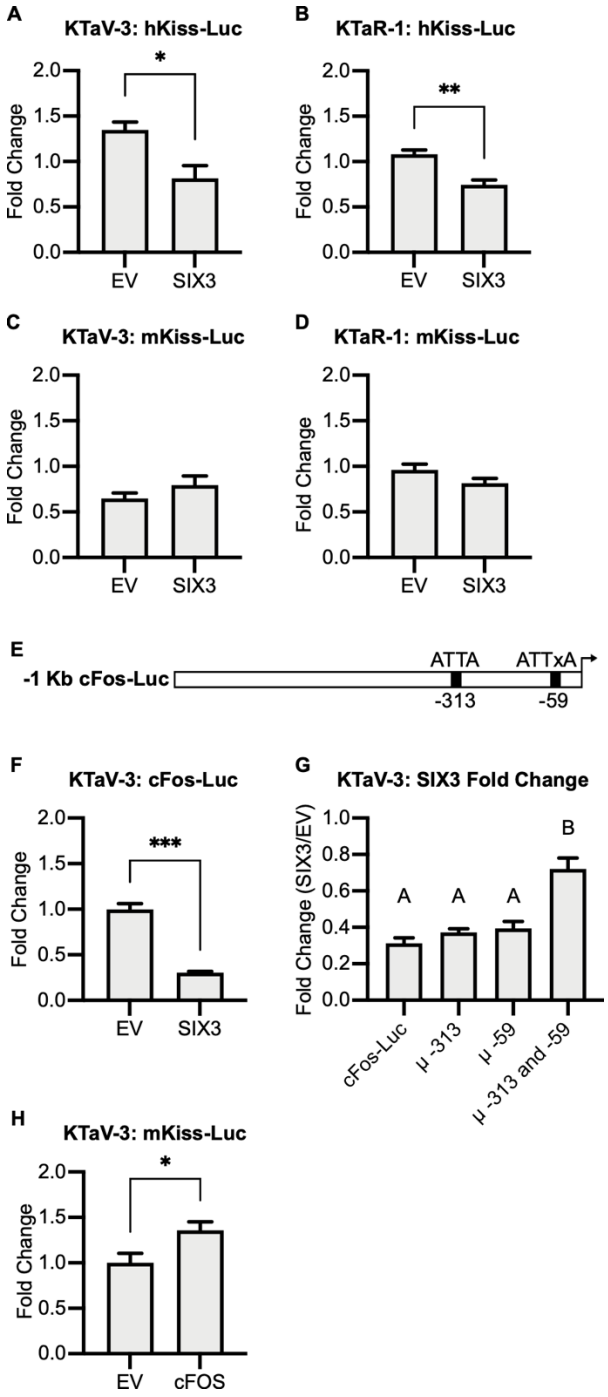

Figure 2.7: SIX3 represses cFos-Luc transcription *in vitro*. hKiss-Luc was co-transfected with 20 ng SIX3 or empty vector (EV) in **(A)** KTaV-3 and **(B)** KTaR-1 cells. mKiss-Luc was co-transfected with 20 ng SIX3 or EV in **(C)** KTaV-3 and **(D)** KTaR-1 cells. **(E)** Schematic of SIX3 binding sites on the -1 Kb cFos promoter. **(F)** cFos-Luc was co-transfected into KTaV-3 cells with 20 ng SIX3 or EV. **(G)** cFos-Luc or cFos-luc reporters containing *cis*-mutations at -313 (μ -313), -59 (μ -59), or both (μ -313 and -59) base pairs were co-transfected with 20 ng SIX3 or EV. Data is represented as fold change of SIX3/EV. **(H)** mKiss-luc was co-transfected into KTaV-3 cells with 50 ng cFOS or EV. For all experiments, bars represent means ± SEM, N=3-5. Data were analyzed using Student's t-test or One-way ANOVA.

Figure 2.8: Kisspeptin-specific *Six3* is not necessary for reproduction in male mice.(A) Time to pubertal onset determined by preputial separation. **(B)** Weight at preputial separation. **(C)** Total sperm per epididymis. **D)** Percent motile sperm. **(E)** Days for males to plug wildtype females. **(F)** Average number of pups produced per litter when set up with a wildtype female. Serum levels of **(G)** FSH, **(H)** LH, **(I)** and testosterone levels in intact male mice. **(J)** *Kiss1*, **(K)** *Tac2, (***L)** and *Pdyn* gene expression in intact male ARC.

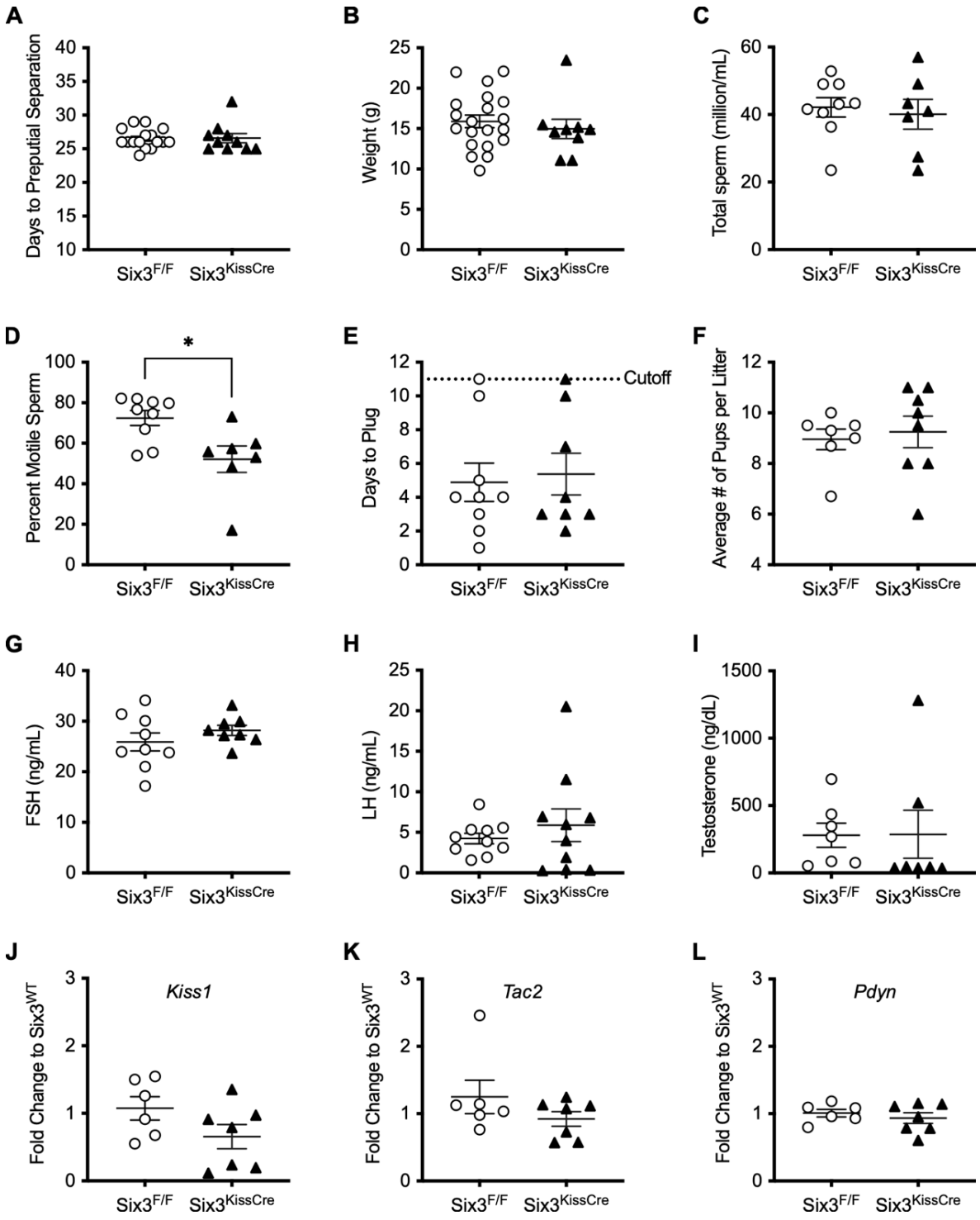
A
Days to Preputial Separation
40
35
30
25
20
15
10
Six3F/F
Six3KissCre
B
Weight (g)
25
20
15
10
5
0
Six3F/F
Six3KissCre
C
Total sperm (million/mL)
60
40
20
0
Six3F/F
Six3KissCre
D
*
Percent Motile Sperm
100
80
60
40
20
0
Six3F/F
Six3KissCre
E
Cutoff
Days to Plug
12
10
8
6
4
2
0
Six3F/F
Six3KissCre
F
Average # of Pups per Litter
12
10
8
6
4
Six3F/F
Six3KissCre
G
FSH (ng/mL)
40
30
20
10
0
Six3F/F
Six3KissCre
H
LH (ng/mL)
25
20
15
10
5
0
Six3F/F
Six3KissCre
I
Testosterone (ng/dL)
1500
1000
500
0
Six3F/F
Six3KissCre
J
Kiss1
Fold Change to Six3WT
3
2
1
0
Six3F/F
Six3KissCre
K
Tac2
Fold Change to Six3WT
3
2
1
0
Six3F/F
Six3KissCre
L
Pdyn
Fold Change to Six3WT
3
2
1
0
Six3F/F
Six3KissCre

References

1. Gottsch ML, Cunningham MJ, Smith JT, Popa SM, Acohido BV, Crowley WF, Seminara S, Clifton DK, Steiner RA. A role for kisspeptins in the regulation of gonadotropin secretion in the mouse. *Endocrinology.* 2004;**145**(9):4073-4077.

2. Irwig MS, Fraley GS, Smith JT, Acohido BV, Popa SM, Cunningham MJ, Gottsch ML, Clifton DK, Steiner RA. Kisspeptin activation of gonadotropin releasing hormone neurons and regulation of KiSS-1 mRNA in the male rat. *Neuroendocrinology.* 2004;**80**(4):264-272.

3. Han SK, Gottsch ML, Lee KJ, Popa SM, Smith JT, Jakawich SK, Clifton DK, Steiner RA, Herbison AE. Activation of gonadotropin-releasing hormone neurons by kisspeptin as a neuroendocrine switch for the onset of puberty. *J Neurosci.* 2005;**25**(49):11349-11356.

4. Messager S, Chatzidaki EE, Ma D, Hendrick AG, Zahn D, Dixon J, Thresher RR, Malinge I, Lomet D, Carlton MB, Colledge WH, Caraty A, Aparicio SA. Kisspeptin directly stimulates gonadotropin-releasing hormone release via G protein-coupled receptor 54. *Proc Natl Acad Sci USA.* 2005;**102**(5):1761-1766.

5. Matsuda F, Ohkura S, Magata F, Munetomo A, Chen J, Sato M, Inoue N, Uenoyama Y, Tsukamura H. Role of kisspeptin neurons as a GnRH surge generator: Comparative aspects in rodents and non-rodent mammals. *J Obstet Gynaecol Res.* 2019;**45**(12):2318-2329.

6. Plant TM. 60 YEARS OF NEUROENDOCRINOLOGY: The hypothalamo-pituitary-gonadal axis. *J Endocrinol.* 2015;**226**(2):T41-54.

7. Kaprara A, Huhtaniemi IT. The hypothalamus-pituitary-gonad axis: Tales of mice and men. *Metabolism.* 2018;**86**:3-17.

8. Stamatiades GA, Kaiser UB. Gonadotropin regulation by pulsatile GnRH: Signaling and gene expression. *Mol Cell Endocrinol.* 2017

9. Kauffman AS. Coming of age in the kisspeptin era: sex differences, development, and puberty. *Mol Cell Endocrinol.* 2010;**324**(1-2):51-63.

10. Topaloglu AK, Tello JA, Kotan LD, Ozbek MN, Yilmaz MB, Erdogan S, Gurbuz F, Temiz F, Millar RP, Yuksel B. Inactivating KISS1 mutation and hypogonadotropic hypogonadism. *N Engl J Med.* 2012;**366**(7):629-635.

11. Topaloglu AK. Update on the Genetics of Idiopathic Hypogonadotropic Hypogonadism. *J Clin Res Pediatr Endocrinol.* 2017;**9**(Suppl 2):113-122.

12. Gottsch ML, Clifton DK, Steiner RA. Kisspepeptin-GPR54 signaling in the neuroendocrine reproductive axis. *Mol Cell Endocrinol.* 2006;**254-255**:91-96.

13. Goodman RL, Lehman MN, Smith JT, Coolen LM, de Oliveira CV, Jafarzadehshirazi MR, Pereira A, Iqbal J, Caraty A, Ciofi P, Clarke IJ. Kisspeptin neurons in the arcuate nucleus

of the ewe express both dynorphin A and neurokinin B. *Endocrinology.* 2007;**148**(12):5752-5760.

14. Wakabayashi Y, Nakada T, Murata K, Ohkura S, Mogi K, Navarro VM, Clifton DK, Mori Y, Tsukamura H, Maeda K, Steiner RA, Okamura H. Neurokinin B and dynorphin A in kisspeptin neurons of the arcuate nucleus participate in generation of periodic oscillation of neural activity driving pulsatile gonadotropin-releasing hormone secretion in the goat. *J Neurosci.* 2010;**30**(8):3124-3132.

15. Moore AM, Lucas KA, Goodman RL, Coolen LM, Lehman MN. Three-dimensional imaging of KNDy neurons in the mammalian brain using optical tissue clearing and multiple-label immunocytochemistry. *Sci Rep.* 2018;**8**(1):2242.

16. Navarro VM, Gottsch ML, Chavkin C, Okamura H, Clifton DK, Steiner RA. Regulation of gonadotropin-releasing hormone secretion by kisspeptin/dynorphin/neurokinin B neurons in the arcuate nucleus of the mouse. *J Neurosci.* 2009;**29**(38):11859-11866.

17. Clarkson J, Han SY, Piet R, McLennan T, Kane GM, Ng J, Porteous RW, Kim JS, Colledge WH, Iremonger KJ, Herbison AE. Definition of the hypothalamic GnRH pulse generator in mice. *Proc Natl Acad Sci U S A.* 2017;**114**(47):E10216-E10223.

18. Smith JT, Cunningham MJ, Rissman EF, Clifton DK, Steiner RA. Regulation of Kiss1 gene expression in the brain of the female mouse. *Endocrinology.* 2005;**146**(9):3686-3692.

19. Smith JT, Dungan HM, Stoll EA, Gottsch ML, Braun RE, Eacker SM, Clifton DK, Steiner RA. Differential regulation of KiSS-1 mRNA expression by sex steroids in the brain of the male mouse. *Endocrinology.* 2005;**146**(7):2976-2984.

20. McQuillan HJ, Han SY, Cheong I, Herbison AE. GnRH Pulse Generator Activity Across the Estrous Cycle of Female Mice. *Endocrinology.* 2019;**160**(6):1480-1491.

21. Dror T, Franks J, Kauffman AS. Analysis of multiple positive feedback paradigms demonstrates a complete absence of LH surges and GnRH activation in mice lacking Kisspeptin signaling. *Biol Reprod.* 2013;**88**(6):146.

22. Dungan HM, Gottsch ML, Zeng H, Gragerov A, Bergmann JE, Vassilatis DK, Clifton DK, Steiner RA. The role of kisspeptin-GPR54 signaling in the tonic regulation and surge release of gonadotropin-releasing hormone/luteinizing hormone. *J Neurosci.* 2007;**27**(44):12088-12095.

23. Hoffmann HM, Pandolfi EC, Larder R, Mellon PL. Haploinsufficiency of homeodomain proteins Six3, Vax1, and Otx2 causes subfertility in mice via distinct mechanisms. *Neuroendocrinology.* 2019;**109**(3):200-207.

24. Hoffmann HM, Tamrazian A, Xie H, Perez-Millan MI, Kauffman AS, Mellon PL. Heterozygous deletion of ventral anterior homeobox (vax1) causes subfertility in mice. *Endocrinology.* 2014;**155**(10):4043-4053.

25. Pandolfi EC, Breuer JA, Nguyen Huu VA, Talluri T, Nguyen D, Lee JS, Hu R, Bharti K, Skowronska-Krawczyk D, Gorman MR, Mellon PL, Hoffmann HM. The homeodomain transcription factors Vax1 and Six6 are required for SCN development and function. *Mol Neurobiol.* 2020;**57**(2):1217-1232.

26. Hoffmann H, Meadows J, Breuer J, Yaw A, Nguyen D, Tonsfeldt K, Chin A, Devries B, Trang C, Oosterhouse H, Lee J, Doser J, Gorman M, Wesh D, Mellon P. The transcription factors SIX3 and VAX1 are required for suprachiasmatic nucleus circadian output and fertility in female mice. *Journal of Neuroscience Research.* 2021;**In Press**(

27. Pandolfi EC, Hoffmann HM, Schoeller EL, Gorman MR, Mellon PL. Haploinsufficiency of SIX3 abolishes male reproductive behavior rhrough disrupted olfactory development, and impairs female fertility through disrupted GnRH neuron migration. *Mol Neurobiol.* 2018;**55**(11):8709-8727.

28. Pandolfi EC, Tonsfeldt KJ, Hoffmann HM, Mellon PL. Deletion of the homeodomain protein Six6 from GnRH neurons decreases GnRH gene expression, resulting in infertility. *Endocrinology.* 2019;**160**(9):2151-2164.

29. Hallonet M, Hollemann T, Wehr R, Jenkins NA, Copeland NG, Pieler T, Gruss P. Vax1 is a novel homeobox-containing gene expressed in the developing anterior ventral forebrain. *Development.* 1998;**125**(14):2599-2610.

30. Hoffmann HM, Trang C, Gong P, Kimura I, Pandolfi EC, Mellon PL. Deletion of Vax1 from gonadotropin-releasing hormone (GnRH) neurons abolishes GnRH rxpression and leads to hypogonadism and infertility. *J Neurosci.* 2016;**36**(12):3506-3518.

31. Hoffmann HM, Mellon PL. A small population of hypothalamic neurons govern fertility: the critical role of VAX1 in GnRH neuron development and fertility maintenance. *Neurosci Commun (Houst).* 2016;**2**:e1373.

32. Cravo RM, Margatho LO, Osborne-Lawrence S, Donato J, Jr., Atkin S, Bookout AL, Rovinsky S, Frazao R, Lee CE, Gautron L, Zigman JM, Elias CF. Characterization of Kiss1 neurons using transgenic mouse models. *Neuroscience.* 2011;**173**:37-56.

33. Madisen L, Zwingman TA, Sunkin SM, Oh SW, Zariwala HA, Gu H, Ng LL, Palmiter RD, Hawrylycz MJ, Jones AR, Lein ES, Zeng H. A robust and high-throughput Cre reporting and characterization system for the whole mouse brain. *Nat Neurosci.* 2010;**13**(1):133-140.

34. Di Giorgio NP, Catalano PN, Lopez PV, Gonzalez B, Semaan SJ, Lopez GC, Kauffman AS, Rulli SB, Somoza GM, Bettler B, Libertun C, Lux-Lantos VA. Lack of functional GABAB receptors alters Kiss1 , Gnrh1 and Gad1 mRNA expression in the medial basal hypothalamus at postnatal day 4. *Neuroendocrinology.* 2013;**98**(3):212-223.

35. Tonsfeldt KJ, Schoeller EL, Brusman LE, Cui LJ, Lee J, Mellon PL. The contribution of the dircadian gene Bmal1 to female fertility and the generation of the preovulatory Luteinizing Hormone surge. *J Endocr Soc.* 2019;**3**(4):716-733.

36. Livak KJ, Schmittgen TD. Analysis of relative gene expression data using real-time quantitative PCR and the 2(-Delta Delta C(T)) Method. *Methods.* 2001;**25**(4):402-408.

37. Gottsch ML, Popa SM, Lawhorn JK, Qiu J, Tonsfeldt KJ, Bosch MA, Kelly MJ, Ronnekleiv OK, Sanz E, McKnight GS, Clifton DK, Palmiter RD, Steiner RA. Molecular properties of Kiss1 neurons in the arcuate nucleus of the mouse. *Endocrinology.* 2011;**152**(11):4298-4309.

38. Schoeller EL, Clark DD, Dey S, Cao NV, Semaan SJ, Chao LW, Kauffman AS, Stowers L, Mellon PL. Bmal1 Is Required for Normal Reproductive Behaviors in Male Mice. *Endocrinology.* 2016;**157**(12):4914-4929.

39. Jacobs DC, Veitch RE, Chappell PE. Evaluation of Immortalized AVPV- and Arcuate-Specific Neuronal Kisspeptin Cell Lines to Elucidate Potential Mechanisms of Estrogen Responsiveness and Temporal Gene Expression in Females. *Endocrinology.* 2016;**157**(9):3410-3419.

40. Mueller JK, Dietzel A, Lomniczi A, Loche A, Tefs K, Kiess W, Danne T, Ojeda SR, Heger S. Transcriptional regulation of the human KiSS1 gene. *Mol Cell Endocrinol.* 2011;**342**(1-2):8-19.

41. Ikonen T, Palvimo JJ, Janne OA. Heterodimerization is mainly responsible for the dominant negative activity of amino-terminally truncated rat androgen receptor forms. *FEBS Lett.* 1998;**430**(3):393-396.

42. Givens ML, Rave-Harel N, Goonewardena VD, Kurotani R, Berdy SE, Swan CH, Rubenstein JL, Robert B, Mellon PL. Developmental regulation of gonadotropin-releasing hormone gene expression by the MSX and DLX homeodomain protein families. *J Biol Chem.* 2005;**280**(19):19156-19165.

43. Schindelin J, Arganda-Carreras I, Frise E, Kaynig V, Longair M, Pietzsch T, Preibisch S, Rueden C, Saalfeld S, Schmid B, Tinevez JY, White DJ, Hartenstein V, Eliceiri K, Tomancak P, Cardona A. Fiji: an open-source platform for biological-image analysis. *Nat Methods.* 2012;**9**(7):676-682.

44. Byers SL, Wiles MV, Dunn SL, Taft RA. Mouse estrous cycle identification tool and images. *PLoS One.* 2012;**7**(4):e35538.

45. Allen Institute for Brain Science 2011 Allen Mouse Brain Atlas. https://mouse.brain-map.org/gene/show/22083. February 2021. In:

46. Ikeda Y, Tagami A, Komada M, Takahashi M. Expression of Kisspeptin in Gonadotrope Precursors in the Mouse Pituitary during Embryonic and Postnatal Development and in Adulthood. *Neuroendocrinology.* 2017;**105**(4):357-371.

47. Salehi S, Adeshina I, Chen H, Zirkin BR, Hussain MA, Wondisford F, Wolfe A, Radovick S. Developmental and endocrine regulation of kisspeptin expression in mouse Leydig cells. *Endocrinology.* 2015;**156**(4):1514-1522.

48. Merhi Z, Thornton K, Bonney E, Cipolla MJ, Charron MJ, Buyuk E. Ovarian kisspeptin expression is related to age and to monocyte chemoattractant protein-1. *J Assist Reprod Genet.* 2016;**33**(4):535-543.

49. Marraudino M, Miceli D, Farinetti A, Ponti G, Panzica G, Gotti S. Kisspeptin innervation of the hypothalamic paraventricular nucleus: sexual dimorphism and effect of estrous cycle in female mice. *J Anat.* 2017;**230**(6):775-786.

50. Wang L, DeFazio RA, Moenter SM. Excitability and burst generation of AVPV kisspeptin neurons are regulated by the estrous cycle via multiple conductances modulated by estradiol action. *eNeuro.* 2016;**3**(3):ENEURO.0094-0016.2016.

51. Ho Y, Hu P, Peel MT, Chen S, Camara PG, Epstein DJ, Wu H, Liebhaber SA. Single-cell transcriptomic analysis of adult mouse pituitary reveals sexual dimorphism and physiologic demand-induced cellular plasticity. *Protein Cell.* 2020;**11**(8):565-583.

52. Steyn FJ, Wan Y, Clarkson J, Veldhuis JD, Herbison AE, Chen C. Development of a methodology for and assessment of pulsatile luteinizing hormone secretion in juvenile and adult male mice. *Endocrinology.* 2013;**154**(12):4939-4945.

53. Kumar TR, Wang Y, Lu N, Matzuk MM. Follicle stimulating hormone is required for ovarian follicle maturation but not male fertility. *Nat Genet.* 1997;**15**(2):201-204.

54. Schurmann A, Koling S, Jacobs S, Saftig P, Krauss S, Wennemuth G, Kluge R, Joost HG. Reduced sperm count and normal fertility in male mice with targeted disruption of the ADP-ribosylation factor-like 4 (Arl4) gene. *Mol Cell Biol.* 2002;**22**(8):2761-2768.

55. Anjum S, Krishna A, Sridaran R, Tsutsui K. Localization of gonadotropin-releasing hormone (GnRH), gonadotropin-inhibitory hormone (GnIH), kisspeptin and GnRH receptor and their possible roles in testicular activities from birth to senescence in mice. *J Exp Zool A Ecol Genet Physiol.* 2012;**317**(10):630-644.

56. Hsu MC, Wang JY, Lee YJ, Jong DS, Tsui KH, Chiu CH. Kisspeptin modulates fertilization capacity of mouse spermatozoa. *Reproduction.* 2014;**147**(6):835-845.

57. Toolee H, Rastegar T, Solhjoo S, Mortezaee K, Mohammadipour M, Kashani IR, Akbari M. Roles for Kisspeptin in proliferation and differentiation of spermatogonial cells isolated from mice offspring when the cells are cocultured with somatic cells. *J Cell Biochem.* 2019;**120**(4):5042-5054.

58. Sharma A, Thaventhiran T, Minhas S, Dhillo WS, Jayasena CN. Kisspeptin and Testicular Function-Is it Necessary? *Int J Mol Sci.* 2020;**21**(8

59. Sanz E, Evanoff R, Quintana A, Evans E, Miller JA, Ko C, Amieux PS, Griswold MD, McKnight GS. RiboTag Analysis of Actively Translated mRNAs in Sertoli and Leydig Cells In Vivo. *PLoS One.* 2013;**8**(6):e66179.

60. Ge R, Chen G, Hardy MP 2009 The Role of the Leydig Cell in Spermatogenic Function. In: C.Y. C ed. Molecular Mechanisms in Spermatogenesis Springer, New York, NY: Advances in Experimental Medicine and Biology

61. Zirkin BR, Papadopoulos V. Leydig cells: formation, function, and regulation. *Biol Reprod.* 2018;**99**(1):101-111.

62. Andersson AM, Jorgensen N, Frydelund-Larsen L, Rajpert-De Meyts E, Skakkebaek NE. Impaired Leydig cell function in infertile men: a study of 357 idiopathic infertile men and 318 proven fertile controls. *J Clin Endocrinol Metab.* 2004;**89**(7):3161-3167.

63. Liu Z, Shi X, Wang L, Yang Y, Fu Q, Tao M. Associations between male reproductive characteristics and the outcome of assisted reproductive technology (ART). *Biosci Rep.* 2017;**37**(3

64. Slavotinek AM, Chao R, Vacik T, Yahyavi M, Abouzeid H, Bardakjian T, Schneider A, Shaw G, Sherr EH, Lemke G, Youssef M, Schorderet DF. VAX1 mutation associated with microphthalmia, corpus callosum agenesis, and orofacial clefting: the first description of a VAX1 phenotype in humans. *Hum Mutat.* 2012;**33**(2):364-368.

65. Kent WJ, Sugnet CW, Furey TS, Roskin KM, Pringle TH, Zahler AM, Haussler D. The human genome browser at UCSC. *Genome Res.* 2002;**12**(6):996-1006.

66. Altschul SF, Madden TL, Schaffer AA, Zhang J, Zhang Z, Miller W, Lipman DJ. Gapped BLAST and PSI-BLAST: a new generation of protein database search programs. *Nucleic Acids Res.* 1997;**25**(17):3389-3402.

67. Robertson JL, Clifton DK, de la Iglesia HO, Steiner RA, Kauffman AS. Circadian regulation of Kiss1 neurons: implications for timing the preovulatory gonadotropin-releasing hormone/luteinizing hormone surge. *Endocrinology.* 2009;**150**(8):3664-3671.

68. Bertuzzi S, Hindges R, Mui SH, O'Leary DD, Lemke G. The homeodomain protein vax1 is required for axon guidance and major tract formation in the developing forebrain. *Genes Dev.* 1999;**13**(23):3092-3105.

69. Semaan SJ, Murray EK, Poling MC, Dhamija S, Forger NG, Kauffman AS. BAX-dependent and BAX-independent regulation of Kiss1 neuron development in mice. *Endocrinology.* 2010;**151**(12):5807-5817.

70. Christian CA, Mobley JL, Moenter SM. Diurnal and estradiol-dependent changes in gonadotropin-releasing hormone neuron firing activity. *Proc Natl Acad Sci USA.* 2005;**102**(43):15682-15687.

71. Bianco SD, Kaiser UB. The genetic and molecular basis of idiopathic hypogonadotropic hypogonadism. *Nat Rev Endocrinol.* 2009;**5**(10):569-576.

72. Au MG, Crowley WF, Jr., Buck CL. Genetic counseling for isolated GnRH deficiency. *Mol Cell Endocrinol.* 2011;**346**(1-2):102-109.

73. Herbison AE. The Gonadotropin-Releasing Hormone Pulse Generator. *Endocrinology.* 2018;**159**(11):3723-3736.

74. Smith JT, Popa SM, Clifton DK, Hoffman GE, Steiner RA. Kiss1 neurons in the forebrain as central processors for generating the preovulatory luteinizing hormone surge. *J Neurosci.* 2006;**26**(25):6687-6694.

75. Lavalle SN, Hoffmann HM, Chou T, Hernandez J, Naing NCP, Tonsfeldt KJ, Mellon PL. Kiss1 is differentially regulated in male and female mice by the homeodomain transcription factor VAX1. . *Mol Cell Endocrinol.* 2021;**in Press**(

76. Conte I, Morcillo J, Bovolenta P. Comparative analysis of Six 3 and Six 6 distribution in the developing and adult mouse brain. *Dev Dyn.* 2005;**234**(3):718-725.

77. Lagutin OV, Zhu CC, Kobayashi D, Topczewski J, Shimamura K, Puelles L, Russell HR, McKinnon PJ, Solnica-Krezel L, Oliver G. Six3 repression of Wnt signaling in the anterior neuroectoderm is essential for vertebrate forebrain development. *Genes Dev.* 2003;**17**(3):368-379.

78. Liu W, Lagutin OV, Mende M, Streit A, Oliver G. Six3 activation of Pax6 expression is essential for mammalian lens induction and specification. *EMBO J.* 2006;**25**(22):5383-5395.

79. RRID:MGI:3693848.

80. RRID:IMSR_JAX:023426.

81. RRID:MGI:104735.

82. RRID:AB_2189178.

83. Hoffmann HM. Determination of reproductive competence by confirming pubertal onset and performing a fertility assay in mice and rats. *J Vis Exp.* 2018140):e58352.

84. Tonsfeldt KJ, Schoeller EL, Brusman LE, Cui LJ, Lee J, Mellon PL. The Contribution of the Circadian Gene Bmal1 to Female Fertility and the Generation of the Preovulatory Luteinizing Hormone Surge. *J Endocr Soc.* 2019;**3**(4):716-733.

85. RRID:CVCL_VS93.

86. RRID:CVCL_VS94.

87. Atkin SD, Owen BM, Bookout AL, Cravo RM, Lee C, Elias CF, Elmquist JK, Kliewer SA, Mangelsdorf DJ. Nuclear receptor LRH-1 induces the reproductive neuropeptide kisspeptin in the hypothalamus. *Mol Endocrinol.* 2013;**27**(4):598-605.

88. Ely HA, Mellon PL, Coss D. GnRH induces the c-Fos gene via phosphorylation of SRF by the calcium/calmodulin kinase II pathway. *Mol Endocrinol.* 2011;**25**(4):669-680.

89. Hoffmann HM, Gong P, Tamrazian A, Mellon PL. Transcriptional interaction between cFOS and the homeodomain-binding transcription factor VAX1 on the GnRH promoter controls Gnrh1 expression levels in a GnRH neuron maturation specific manner. *Mol Cell Endocrinol.* 2018;**461**:143-154.

90. Glidewell-Kenney CA, Shao PP, Iyer AK, Grove AM, Meadows JD, Mellon PL. Neurokinin B causes acute GnRH secretion and repression of GnRH transcription in GT1-7 GnRH neurons. *Mol Endocrinol.* 2013;**27**(3):437-454.

91. Teles MG, Bianco SD, Brito VN, Trarbach EB, Kuohung W, Xu S, Seminara SB, Mendonca BB, Kaiser UB, Latronico AC. A GPR54-activating mutation in a patient with central precocious puberty. *N Engl J Med.* 2008;**358**(7):709-715.

92. de Roux N, Genin E, Carel JC, Matsuda F, Chaussain JL, Milgrom E. Hypogonadotropic hypogonadism due to loss of function of the KiSS1-derived peptide receptor GPR54. *Proc Natl Acad Sci USA.* 2003;**100**(19):10972-10976.

93. Seminara SB, Messager S, Chatzidaki EE, Thresher RR, Acierno JS, Jr., Shagoury JK, Bo-Abbas Y, Kuohung W, Schwinof KM, Hendrick AG, Zahn D, Dixon J, Kaiser UB, Slaugenhaupt SA, Gusella JF, O'Rahilly S, Carlton MB, Crowley WF, Jr., Aparicio SA, Colledge WH. The GPR54 gene as a regulator of puberty. *N Engl J Med.* 2003;**349**(17):1614-1627.

94. Smith JT. Kisspeptin signalling in the brain: steroid regulation in the rodent and ewe. *Brain Res Rev.* 2008;**57**(2):288-298.

95. Smith JT. Sex steroid regulation of kisspeptin circuits. *Adv Exp Med Biol.* 2013;**784**:275-295.

96. Kawakami K, Sato S, Ozaki H, Ikeda K. Six family genes--structure and function as transcription factors and their roles in development. *Bioessays.* 2000;**22**(7):616-626.

97. Yue F, Cheng Y, Breschi A, Vierstra J, Wu W, Ryba T, Sandstrom R, Ma Z, Davis C, Pope BD, Shen Y, Pervouchine DD, Djebali S, Thurman RE, Kaul R, Rynes E, Kirilusha A, Marinov GK, Williams BA, Trout D, Amrhein H, Fisher-Aylor K, Antoshechkin I, DeSalvo G, See LH, Fastuca M, Drenkow J, Zaleski C, Dobin A, Prieto P, Lagarde J, Bussotti G, Tanzer A, Denas O, Li K, Bender MA, Zhang M, Byron R, Groudine MT, McCleary D, Pham L, Ye Z, Kuan S, Edsall L, Wu YC, Rasmussen MD, Bansal MS, Kellis M, Keller CA, Morrissey CS, Mishra T, Jain D, Dogan N, Harris RS, Cayting P, Kawli T, Boyle AP, Euskirchen G, Kundaje A, Lin S, Lin Y, Jansen C, Malladi VS, Cline MS, Erickson DT, Kirkup VM, Learned K, Sloan CA, Rosenbloom KR, Lacerda de Sousa B, Beal K, Pignatelli M, Flicek P, Lian J, Kahveci T, Lee D, Kent WJ, Ramalho Santos M, Herrero J, Notredame C, Johnson A, Vong S, Lee K, Bates D, Neri F, Diegel M, Canfield T, Sabo PJ, Wilken MS, Reh TA, Giste E, Shafer A, Kutyavin T, Haugen E, Dunn D, Reynolds AP, Neph S, Humbert R, Hansen RS, De Bruijn M, Selleri L, Rudensky A, Josefowicz S, Samstein R, Eichler EE, Orkin SH, Levasseur D, Papayannopoulou T, Chang KH, Skoultchi A, Gosh S, Disteche C, Treuting P, Wang Y, Weiss MJ, Blobel GA, Cao X, Zhong S, Wang T, Good PJ, Lowdon RF, Adams LB, Zhou XQ, Pazin MJ, Feingold EA, Wold B, Taylor J, Mortazavi A, Weissman SM, Stamatoyannopoulos JA, Snyder MP, Guigo R, Gingeras TR, Gilbert

DM, Hardison RC, Beer MA, Ren B, Mouse EC. A comparative encyclopedia of DNA elements in the mouse genome. *Nature.* 2014;**515**(7527):355-364.

98. de la Iglesia HO, Schwartz WJ. Minireview: timely ovulation: circadian regulation of the female hypothalamo-pituitary-gonadal axis. *Endocrinology.* 2006;**147**(3):1148-1153.

99. Hoffman GE, Smith MS, Verbalis JG. c-Fos and related immediate early gene products as markers of activity in neuroendocrine systems. *Front Neuroendocrinol.* 1993;**14**(3):173-213.

100. Kovacs KJ. Measurement of immediate-early gene activation- c-fos and beyond. *J Neuroendocrinol.* 2008;**20**(6):665-672.

101. Karin M, Liu Z, Zandi E. AP-1 function and regulation. *Curr Opin Cell Biol.* 1997;**9**(2):240-246.

102. Coss D, Jacobs SB, Bender CE, Mellon PL. A novel AP-1 site is critical for maximal induction of the follicle-stimulating hormone beta gene by gonadotropin-releasing hormone. *J Biol Chem.* 2004;**279**(1):152-162.

103. Jeong KH, Chin WW, Kaiser UB. Essential role of the homeodomain for pituitary homeobox 1 activation of mouse gonadotropin-releasing hormone receptor gene expression through interactions with c-Jun and DNA. *Mol Cell Biol.* 2004;**24**(14):6127-6139.

104. Xie C, Jonak CR, Kauffman AS, Coss D. Gonadotropin and kisspeptin gene expression, but not GnRH, are impaired in cFOS deficient mice. *Mol Cell Endocrinol.* 2015;**411**:223-231.

105. Norwitz ER, Xu S, Xu J, Spiryda LB, Park JS, Jeong KH, McGee EA, Kaiser UB. Direct binding of AP-1 (Fos/Jun) proteins to a SMAD binding element facilitates both GnRH- and activin-mediated transcriptional activation of the mouse GnRH receptor gene. *J Biol Chem.* 2002;**277**(40):37469-37478.

106. Sharma SC, Richards JS. Regulation of AP1 (Jun/Fos) factor expression and activation in ovarian granulosa cells. Relation of JunD and Fra2 to terminal differentiation. *J Biol Chem.* 2000;**275**(43):33718-33728.

107. Piet R, Fraissenon A, Boehm U, Herbison AE. Estrogen permits vasopressin signaling in preoptic kisspeptin neurons in the female mouse. *J Neurosci.* 2015;**35**(17):6881-6892.

108. Christian CA, Moenter SM. The neurobiology of preovulatory and estradiol-induced gonadotropin-releasing hormone surges. *Endocr Rev.* 2010;**31**(4):544-577.

109. Hoffmann HM, Meadows JD, Breuer JA, Yaw AM, Nguyen D, Tonsfeldt KJ, Chin AY, Devries BM, Trang C, Oosterhouse HJ, Lee JS, Doser JW, Gorman MR, Wesh DK, Mellon PL. The transcription factors SIX3 and VAX1 are required for suprachiasmatic nucleus circadian output and fertility in female mice. *Journal of Neuroscience Research.* 2021;**in press**(

110. Zhu CC, Dyer MA, Uchikawa M, Kondoh H, Lagutin OV, Oliver G. Six3-mediated auto repression and eye development requires its interaction with members of the Groucho-related family of co-repressors. *Development.* 2002;**129**(12):2835-2849.

111. Manavathi B, Peng S, Rayala SK, Talukder AH, Wang MH, Wang RA, Balasenthil S, Agarwal N, Frishman LJ, Kumar R. Repression of Six3 by a corepressor regulates rhodopsin expression. *Proc Natl Acad Sci U S A.* 2007;**104**(32):13128-13133.